RKDG methods with WENO type limiters and conservative interfacial procedure for one-dimensional compressible multi-medium flow simulations ☆

Jun Zhu [a,b], Jianxian Qiu [c,d], Tiegang Liu [e], Boo Cheong Khoo [f,a,∗]

[a] *Singapore–MIT Alliance, 4 Engineering Drive 3, National University of Singapore, Singapore 117576, Singapore*
[b] *College of Science, Nanjing University of Aeronautics and Astronautics, Nanjing, Jiangsu 210016, PR China*
[c] *Department of Mathematics, Nanjing University, Nanjing, Jiangsu 210093, PR China*
[d] *School of Mathematical Sciences, Xiamen University, Xiamen, Fujian 361005, PR China*
[e] *LMIB and School of Mathematics and System Sciences, Beijing University of Aeronautics and Astronautics, Beijing 100191, PR China*
[f] *Department of Mechanical Engineering, National University of Singapore, Singapore 119260, Singapore*

A R T I C L E   I N F O

A B S T R A C T

In this paper, we continue on studying the Runge–Kutta discontinuous Galerkin (RKDG) methods to solve compressible multi-medium flow with conservative treatment of the moving material interface. Comparing with the paper by J. Qiu, T.G. Liu and B.C. Khoo [J. Comput. Phys. 222 (2007) 353–373], we adopt the HLLC flux instead of Lax-Friedrichs numerical flux, the finite volume weighted essentially nonoscillatory (WENO) and Hermite WENO (HWENO) reconstructions as limiter instead of TVB limiter for RKDG. The HLLC flux is based on the approximate Riemann solver with little numerical viscosity and can resolve the contact discontinuity and shear wave very well. For limiter procedure, first we use the KXRCF indicator to identify the troubled cell, then apply WENO or HWENO method to reconstruct the polynomial in the troubled cell, while maintaining the cell average. This limiter procedure is more accurate and less problem dependent than the TVB limiter. Numerical results in one dimension for multi-medium flows such as gas–gas and gas–water are provided to illustrate the capability of these procedures.

© 2011 IMACS. Published by Elsevier B.V. All rights reserved.

1. Introduction

In this paper, we continue on studying the Runge–Kutta discontinuous Galerkin (RKDG) methods to solve compressible two-medium flow with conservative treatment of the moving material interface. In general, algorithms proposed for solving two-medium compressible flow consist of two parts. One is the method for solving the single-medium flow and the other is to treat the interface of the two fluids. In [23], Qiu et al. applied RKDG methods to solve the single-medium flow and developed a conservative treatment of the moving material interfaces for compressible two-medium flow. The RKDG methods have been widely applied and performed very well to solve the single-medium compressible flow for past 20 years. The first discontinuous Galerkin (DG) method was introduced by Reed and Hill [30]. A major development of the DG method was carried out by Cockburn et al. in a series of papers [8–12], in which they established a framework to solve for the nonlinear time dependent hyperbolic conservation laws. They employed the explicit, nonlinearly stable high-order Runge–

∗ Corresponding author at: Department of Mechanical Engineering, National University of Singapore, Singapore 119260, Singapore.
E-mail addresses: smazj@nus.edu.sg, zhujun@nuaa.edu.cn (J. Zhu), jxqiu@nju.edu.cn, jxqiu@xmu.edu.cn (J. Qiu), liutg@buaa.edu.cn (T. Liu), mpekbc@nus.edu.sg (B.C. Khoo).

Kutta time discretizations [33] and DG discretization in space with exact or approximate Riemann solvers as interface fluxes and total variation bounded (TVB) limiter [31] to achieve nonoscillatory properties for strong shocks. These schemes are termed RKDG methods.

There are two important components of RKDG methods for solving the conservation laws. One is the nonlinear limiter, which is applied to detect discontinuities and control spurious oscillations near discontinuities. The other is the numerical flux, based on exact or approximate Riemann solvers, which are borrowed from finite difference and finite volume methodologies.

For the nonlinear limiters, there are many limiters presented in the literature, such as the minmod type TVB limiter [8–12], which is a slope limiter using a technique borrowed from the finite volume methodology; the moment based limiter [3] and an improved moment limiter [5], which are specifically designed for DG methods and work on the moments of the numerical solution. Such limiters may be used to control spurious oscillations and maintain the proper order of accuracy in the smooth regions at the same time. But these purposes are usually difficult to achieve in a robust way. And these limiters may degrade in numerical accuracy when mistakenly used in the smooth regions of the solution. On the other hand, the weighted essentially nonoscillatory (WENO) or Hermite WENO (HWENO) method [14,19,32,36] has been developed in the context of finite volume and finite difference frameworks to successfully achieve both uniform high-order accuracy and sharp, essentially nonoscillatory shock transitions. The WENO or HWENO methodology is more robust than the slope limiter methodology, especially for the high-order schemes. Thus it would be natural to try to use the WENO or HWENO methodology as limiters for the discontinuous Galerkin methods. Recently, Qiu and his colleagues [25–27,37,38] developed WENO [14,19,32] and HWENO [36] type methodology as limiters for RKDG methods with the following framework adopted:

Step 1: First, identify the "troubled cells", namely those cells which might need the limiting procedure.

Step 2: Then, replace the solution polynomials in those "troubled cells" by reconstructed polynomials using the WENO or HWENO reconstruction methodology which maintains the original cell averages (conservation), and retains the same orders of accuracy as before, but are much less oscillatory.

This technique works quite well when applied to computing the single-medium compressible problems in one and two dimensions. In [28], Qiu and Shu, had systematically studied and compared a few different troubled-cell indicators for the RKDG methods using WENO methodology as limiters. They showed that the KXRCF indicator by Krivodonova et al. [17] was a suitable candidate for applications of the RKDG methods using WENO reconstructions, which is designed based on a strong superconvergence at the outflow boundary of each element in smooth regions for the DG method.

For the numerical flux, in [29], Qiu et al. have systematically studied and compared a few different fluxes for the RKDG methods. The conclusion based on extensive one and two-dimensional simulations on the hyperbolic systems of Euler equations indicates that the HLLC flux [35] might be a good choice as flux for the RKDG method when all factors such as the cost of CPU time, numerical errors and resolution of discontinuities in the solution are considered.

The treatment of the moving material interfaces and their immediate vicinities is a relatively dominant difficulty for simulating the compressible multi-medium flow. There can arise severe nonphysical oscillations in the vicinity of the material interface especially in the presence of shock or large density ratio even if the well established numerical methods for the single-medium flow are applied directly to the multi-medium flow. There were several works on how to deal with this difficulty [1,2,4,7,15,18,21]. In the fairly recent times, the ghost fluid method (GFM) [13] has provided a flexible way to treat the material interface reasonably well although nonconservatively. It is easy to solve for multi-dimensional cases. Since only single fluid flux formulations are required for the GFM, the proposed method can be employed directly for any two fluids of vastly different equation of states [6,24]. There are subsequent variations of the original GFM with other applications [2,16]. On the other hand, it is precisely the manner of treatment of the single-medium across the material interface by GFM which may cause numerical inaccuracy especially when there is a strong shock wave interaction with the material interface; this had led to the modified GFM [20,22]. In [23], Qiu et al. developed the DG technique to treat the moving material interfaces conservatively.

In this paper, following up the work of [23], we continue our study of the RKDG methods to solve compressible two-medium flow with conservative treatment of the moving material interface. Comparing with the paper [23], we adopt the HLLC flux instead of Lax-Friedrichs numerical flux, the finite volume weighted essentially nonoscillatory (WENO) and Hermite WENO (HWENO) reconstructions as limiter instead of TVB limiter for RKDG. The HLLC flux is based on the approximate Riemann solver with little numerical viscosity and can resolve the contact discontinuity and shear wave very well. For limiter procedure, first we use the KXRCF indicator to identify the troubled cell, then apply WENO or HWENO method to reconstruct the polynomial in the troubled cell, while maintaining the cell average. This limiter procedure is more accurate and less problem dependent than the TVB limiter.

The focus of the paper is on the development of limiter procedure on the interface of two fluids. We present the detailed procedures for the WENO and HWENO reconstructions for the "troubled cells" located at different positions with respect to the material interface: when the "troubled cells" are far away from the material interface and the reconstructions' stencils do not contain the interfacial cells, the formulations are unchanged like for the single-medium computations (we shall define them as regular cells); when the "troubled cells" are the interfacial cells or the reconstructions' stencils involve the interfacial cells, the formulations are changed and we first solve for the Riemann problem at the material interface, then employ the isobaric fix [13] to get the variables of the other material interface side cells. In doing so, we have the WENO3-RKDG2, WENO5-RKDG3 and HWENO5-RKDG3 schemes in conjunction with the conservative material interface treatment [23] for multi-medium flow simulations in one dimension. The organization of this paper is as follows. In Section 2, we

review and construct the finite volume WENO/HWENO reconstructions as limiters for the RKDG methods, which include the reconstructions for the regular cells and interfacial cells. Extensive numerical tests for the gas–gas and gas–water problems are found in Section 3 to verify these procedures. Concluding remarks are given in Section 4. In Appendices A–D, we give the procedures for the higher-order WENO5/HWENO5 type reconstructions as applied to the regular cell and interfacial cell that are omitted in Section 2.

2. WENO and HWENO reconstructions as limiters for the discontinuous Galerkin methods

In this section, we consider the one-dimensional hyperbolic conservation laws:

$$u_t + f(u)_x = \frac{\partial}{\partial t} \begin{pmatrix} \rho \\ \rho v \\ E \end{pmatrix} + \frac{\partial}{\partial x} \begin{pmatrix} \rho v \\ \rho v^2 + p \\ v(E + p) \end{pmatrix} = 0. \tag{2.1}$$

Here, ρ is the density, v is the velocity, p is the pressure and E (total energy) $\equiv \rho e + \frac{1}{2}\rho v^2$, where e is the specific internal energy per unit mass. For closure of the system, the equation of state (EOS) is required. The γ-law used for gases is given as:

$$\rho e = \frac{p}{\gamma - 1} \tag{2.2}$$

and Tait EOS used for the water medium [13,21] is expressed as:

$$\rho e = \frac{p + N\bar{B}}{N - 1}, \tag{2.3}$$

where $\bar{B} = B - A$, $N = 7.15$, $A = 10^5$ Pa and $B = 3.31 \times 10^8$ Pa.

2.1. WENO and HWENO reconstructions as limiters for application of RKDG methods to regular cell

For simplicity of presentation, we shall assume that the mesh is uniformly distributed into several cells $I_i = [x_{i-1/2}, x_{i+1/2}]$, with the cell size $x_{i+1/2} - x_{i-1/2} = \Delta x = h$, cell center $x_i = \frac{1}{2}(x_{i+1/2} + x_{i-1/2})$. We denote the cell average of u as: $\bar{u}_i(t) = \frac{1}{h}\int_{I_i} u(x,t)\,dx$. The DG solution as well as the test function space is given by $V_h^k = \{p: p|_{I_i} \in P^k(I_i)\}$ and is the polynomial spaces of degree at most k on the cell I_i. We adopt a local orthogonal basis over I_i, $\{v_l^{(i)}(x)(l = 0, 1, \ldots, k)\}$, such as:

$$v_0^{(i)}(x) = 1, \qquad v_1^{(i)}(x) = \frac{x - x_i}{h}, \qquad v_2^{(i)}(x) = \left(\frac{x - x_i}{h}\right)^2 - \frac{1}{12}, \quad \ldots.$$

Then the numerical solution $u^h(x,t)$ in the space V_h^k can be written as $u^h(x,t) = \sum_{l=0}^{k} u_i^{(l)}(t) v_i^{(i)}(x)$, for $x \in I_i$ and the degrees of freedom $u_i^{(l)}(t)$ are the moments defined by $u_i^{(l)}(t) = \frac{1}{\int_{I_i} (v_l^{(i)}(x))^2\,dx}\int_{I_i} u^h(x,t) v_l^{(i)}(x)\,dx$ $(l = 0, \ldots, k)$. In order to determine the approximate solution, we evolve the degrees of freedom $u_i^{(l)}(t)$:

$$\frac{d}{dt} u_i^{(l)}(t) = -\frac{1}{\int_{I_i}(v_l^{(i)}(x))^2\,dx}\left(-\int_{I_i} f(u^h(x,t))\frac{d}{dx}v_l^{(i)}(x)\,dx + \hat{f}(u_{i+1/2}^-, u_{i+1/2}^+)v_l^{(i)}(x_{i+1/2})\right.$$

$$\left. - \hat{f}(u_{i-1/2}^-, u_{i-1/2}^+)v_l^{(i)}(x_{i-1/2})\right) \quad (l = 0, \ldots, k) \tag{2.4}$$

where $u_{i+1/2}^{\pm} = u^h(x_{i+1/2}^{\pm}, t)$ are the left and right limits of the discontinuous solution $u^h(x, t)$ at the cell interface $x_{i+1/2}$, $\hat{f}(u^-, u^+)$ is a monotone flux for the scalar case and an exact or approximate Riemann solver for the system. In this paper, we use the HLLC flux (a modification of the HLL flux) [34,35]. The HLLC flux is based on the approximate Riemann solver with only three constant states separated by two waves while resolving the contact and shear waves. For the Euler equations (2.1), it is given as follows:

$$\hat{f}(u^-, u^+) = \begin{cases} f(u^-) & \text{if } 0 \leqslant s^-, \\ f(u^-) + s^-(u^{*-} - u^-) & \text{if } s^- \leqslant 0 \leqslant s^*, \\ f(u^+) + s^+(u^{*+} - u^+) & \text{if } s^* \leqslant 0 \leqslant s^+, \\ f(u^+) & \text{if } s^+ \leqslant 0, \end{cases} \tag{2.5}$$

where, for the sound speed $c = \sqrt{\gamma p/\rho}$ and $K = \pm$,

$$u^{*K} = \rho^K \frac{s^K - v^K}{s^K - s^*} \begin{pmatrix} 1 \\ s^* \\ E^K/\rho^K + (s^* - v^K)(s^* + p^K/(\rho^K(s^K - v^K))) \end{pmatrix}, \tag{2.6}$$

$$q^K = \begin{cases} 1 & \text{if } p^* \leqslant p^K, \\ (1 + \frac{\gamma+1}{2\gamma}(p^*/p^K - 1))^{\frac{1}{2}} & \text{if } p^* > p^K, \end{cases} \tag{2.7}$$

with $s^- = v^- - c^- q^-$, $s^* = v^*$, $s^+ = v^+ + c^+ q^+$, $p^* = \frac{1}{2}(p^- + p^+) - \frac{1}{2}(v^+ - v^-)\bar{\rho}\bar{c}$, $v^* = \frac{1}{2}(v^- + v^+) - \frac{p^+ - p^-}{2\bar{\rho}\bar{c}}$, $\bar{\rho} = \frac{1}{2}(\rho^- + \rho^+)$ and $\bar{c} = \frac{1}{2}(c^- + c^+)$.

For the simplicity, we shall denote $u_i^{(*)} = u_i^{(*)}(t)$ in the following text. The limiter adopted here is described below in some details, as it is a shock detection technique by Krivodonova, Xin, Remacle, Chevaugeon and Flaherty (KXRCF) [17] to detect the "troubled cells". In this paper, we use density and energy as detection conservative variables. Next, we partition the boundary of the cell I_i into two portions ∂I_i^- and ∂I_i^+, where the flow is into ($v \cdot \vec{n} < 0$, $\vec{n}$ is the normal vector to ∂I_i) or out of ($v \cdot \vec{n} > 0$) I_i, respectively. Then the cell I_i is identified as a "troubled cell", where:

$$\frac{|\int_{\partial I_i^-}(u^h|_{I_i} - u^h|_{I_{n_i}})\,ds|}{h^{\frac{k+1}{2}}|\partial I_i^-| \|u^h|_{I_i}\|} > 1. \tag{2.8}$$

Here, I_{n_i} is the neighbor of I_i sharing the boundary ∂I_i^- and the norm is based on an element average in one dimension. For the "troubled cells", we reconstruct the polynomial solutions while retaining their cell averages.

For the second-order $k = 1$ case, we summarize the procedure for reconstructing the first moments $u_i^{(1)}$ for "troubled cells" I_i by using WENO3.

2.1.1. WENO3 as limiter for application of RKDG2 (WENO3-RKDG2) to regular cell

Step 1.1. Given the small stencils $S_1 = \{I_{i-1}, I_i\}$, $S_2 = \{I_i, I_{i+1}\}$ and the bigger stencil $\Gamma = S_1 \cup S_2$, we construct the linear reconstruction polynomials $p_n(x) \in span\{1, (x - x_i)/h\}$ $(n = 1, 2)$ and a second degree reconstruction polynomial $q(x) \in span\{1, (x - x_i)/h, (x - x_i)^2/h^2\}$, such that:

$$\frac{1}{h}\int_{I_{i+j}} p_1(x)\,dx = u_{i+j}^{(0)}, \quad j = -1, 0, \tag{2.9}$$

$$\frac{1}{h}\int_{I_{i+j}} p_2(x)\,dx = u_{i+j}^{(0)}, \quad j = 0, 1, \tag{2.10}$$

$$\frac{1}{h}\int_{I_{i+j}} q(x)\,dx = u_{i+j}^{(0)}, \quad j = -1, 0, 1. \tag{2.11}$$

At the point $x_{i+\frac{\sqrt{3}}{6}}$, we have:

$$p_1(x_{i+\frac{\sqrt{3}}{6}}) = (-\sqrt{3}u_{i-1}^{(0)} + (6 + \sqrt{3})u_i^{(0)})/6, \tag{2.12}$$

$$p_2(x_{i+\frac{\sqrt{3}}{6}}) = ((6 - \sqrt{3})u_i^{(0)} + \sqrt{3}u_{i+1}^{(0)})/6. \tag{2.13}$$

At the point $x_{i-\frac{\sqrt{3}}{6}}$, we have:

$$p_1(x_{i-\frac{\sqrt{3}}{6}}) = (\sqrt{3}u_{i-1}^{(0)} + (6 - \sqrt{3})u_i^{(0)})/6, \tag{2.14}$$

$$p_2(x_{i-\frac{\sqrt{3}}{6}}) = ((6 + \sqrt{3})u_i^{(0)} - \sqrt{3}u_{i+1}^{(0)})/6. \tag{2.15}$$

Step 1.2. We find the combination coefficients, also called linear weights, denoted by γ_1, γ_2, which satisfy: $q(x_G) = \sum_{j=1}^2 \gamma_j p_j(x_G)$ where x_G is a Gaussian quadrature point. In this paper, we use the "two-point" quadrature points: $x_{i\pm\frac{\sqrt{3}}{6}} = x_i \pm \frac{\sqrt{3}}{6}h$. Different quadrature points correspond to different linear weights. For $x_G = x_{i+\frac{\sqrt{3}}{6}}$, the associated linear weights are:

$$\gamma_1 = 1/2, \qquad \gamma_2 = 1/2. \tag{2.16}$$

For $x_G = x_{i-\frac{\sqrt{3}}{6}}$, the associated linear weights are:

$$\gamma_1 = 1/2, \qquad \gamma_2 = 1/2. \tag{2.17}$$

Step 1.3. We compute the smoothness indicators β_n $(n = 1, \ldots, k+1)$ for stencils S_n $(n = 1, \ldots, k+1)$. The smoothness indicators are the same for the reconstruction of all Gaussian points in the same cell, thus significantly reducing the computational cost. As in [14], we used the following smoothness indicators:

$$\beta_n = \sum_{\alpha=1}^{k} \int_{I_i} h^{2\alpha-1} \left(\frac{d^\alpha p_n(x)}{dx^\alpha} \right)^2 dx \quad (n = 1, \ldots, k+1). \tag{2.18}$$

Step 1.4. We compute the nonlinear weights based on the smoothness indicators:

$$\omega_n = \frac{\bar{\omega}_n}{\sum_{l=1}^{k+1} \bar{\omega}_l}, \qquad \bar{\omega}_n = \frac{\gamma_n}{\sum_{l=1}^{k+1} (10^{-6} + \beta_l)^2} \quad (n = 1, \ldots, k+1) \tag{2.19}$$

where γ_n $(n = 1, \ldots, k+1)$ are the linear weights determined above. Then the final WENO3 approximations are given by:

$$u(x_G, t) \approx \sum_{n=1}^{k+1} \omega_n p_n(x_G). \tag{2.20}$$

Step 1.5. We obtain the reconstructed moments based on the reconstructed point values $u(x_G, t)$ at the Gaussian quadrature points x_G and a numerical integration:

$$u_i^{(l)}(t) \approx \frac{1}{\sum_G \sigma_G (v_l^{(i)}(x_G))^2} \sum_G \sigma_G u(x_G, t) v_l^{(i)}(x_G) \quad (l = 1). \tag{2.21}$$

Here σ_G is the Gaussian quadrature weight for the point x_G. The polynomial solution in this cell I_i is then obtained by $u^h(x, t) = \sum_{l=0}^{1} u_i^{(l)}(t) v_i^{(i)}(x)$, for $x \in I_i$ with the reconstructed moment $u_i^{(l)}(t)$ $(l = 1)$ and the original cell average $u_i^{(0)}(t)$.

Step 1.6. The semidiscrete scheme is then discretized in time by a TVD Runge–Kutta method [33]. For example, the third-order version:

$$\begin{cases} u^{(1)} = u^n + \Delta t L(u^n), \\ u^{(2)} = \frac{3}{4} u^n + \frac{1}{4} u^{(1)} + \frac{1}{4} \Delta t L(u^{(1)}), \\ u^{n+1} = \frac{1}{3} u^n + \frac{2}{3} u^{(2)} + \frac{2}{3} \Delta t L(u^{(2)}). \end{cases} \tag{2.22}$$

Remark. In this paper, the reconstruction is performed after each inner stage of the TVD Runge–Kutta method. We define the time-step size $\Delta t = \frac{CFL*h}{\max(v)+c}$ for all the examples.

For the third-order $k = 2$ case, we reconstruct the first and second moments $u_i^{(1)}$ and $u_i^{(2)}$ for "troubled cells" I_i using the WENO5 or HWENO5 in [14,25–27,32], which are given in detail in Appendices A–D.

2.2. WENO and HWENO reconstructions as limiters for application of RKDG methods to interfacial cell

We use the level set method [13,23] to compute the location of the interface $x^*(t^{n+1})$ at $t = t^{n+1}$ based on the data at $t = t^n$. Let $x^*(t^n) \in I_i$, then we evolve (2.4) for Fluid I from $l = 1$ to $i-2$ and for Fluid II from $l = i+2$ to the end, respectively. And we also merge the interfacial cells and get two new cells: $\bar{I}_{i-1} = I_{i-1} \cup [x_{i-\frac{1}{2}}, x^*(t^n)]$, $\bar{I}_{i+1} = [x^*(t^n), x_{i+\frac{1}{2}}] \cup I_{i+1}$, and the new moments are denoted by $\bar{u}_*^{(*)}(t^n)$ and $\xi = \frac{x^*(t^n) - x_i}{h} \in [-\frac{1}{2}, \frac{1}{2}]$. The computation for the cells next to the interface was described in details in [23]. We construct the DG methods for Fluid I over the cell $\bar{I}_{i-1}$ and Fluid II over the cell $\bar{I}_{i+1}$ by the formula:
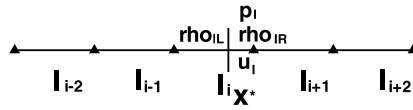
Fig. 2.1. Interfacial cell diagram.

$$\frac{d}{dt} \int_{x_{i-3/2}}^{x^*(t)} u(x,t) v_l^{(i)}(x)\, dx = -\left(f\left(u\left(x^*(t),t\right)\right) - \frac{dx^*(t)}{dt} u\left(x^*(t),t\right) \right) v_l^{(i)}\left(x^*(t)\right)$$

$$+ f\left(u(x_{i-3/2},t)\right) v_l^{(i)}(x_{i-3/2}) + \int_{x_{i-3/2}}^{x^*(t)} f\left(u(x,t)\right) \frac{dv_l^{(i)}(x)}{dx}\, dx \quad (l=0,\ldots,k), \tag{2.23}$$

$$\frac{d}{dt} \int_{x^*(t)}^{x_{i+3/2}} u(x,t) v_l^{(i)}(x)\, dx = \left(f\left(u\left(x^*(t),t\right)\right) - \frac{dx^*(t)}{dt} u\left(x^*(t),t\right) \right) v_l^{(i)}\left(x^*(t)\right)$$

$$- f\left(u(x_{i+3/2},t)\right) v_l^{(i)}(x_{i+3/2}) + \int_{x^*(t)}^{x_{i+3/2}} f\left(u(x,t)\right) \frac{dv_l^{(i)}(x)}{dx}\, dx \quad (l=0,\ldots,k). \tag{2.24}$$

We define the base functions $\{v_l^{(i)}(x)\}$ as continuous over the cell $\bar{I}_{i-1}$ and $\bar{I}_{i+1}$, but cannot maintain the orthogonal property. And these can be written as $u_I^h(x,t) = \sum_{j=0}^{k} u_I^{(j)}(t) v_j^{(i)}(x)$ and $u_{II}^h(x,t) = \sum_{j=0}^{k} u_{II}^{(j)}(t) v_j^{(i)}(x)$. Then we discretize (2.23) and (2.24) as:

$$\frac{d\bar{u}_I^{(l)}(t)}{dt} = -f^*\left(u_I\left(x^*(t),t\right)\right) v_l^{(i)}\left(x^*(t)\right) + f\left(u_I^h(x_{i-3/2},t)\right) v_l^{(i)}(x_{i-3/2}) + \int_{x_{i-3/2}}^{x^*(t)} f\left(u_I^h(x,t)\right) \frac{dv_l^{(i)}(x)}{dx}\, dx \quad (l=0,\ldots,k),$$

$$\tag{2.25}$$

$$\frac{d\bar{u}_{II}^{(l)}(t)}{dt} = f^*\left(u_{II}\left(x^*(t),t\right)\right) v_l^{(i)}\left(x^*(t)\right) - f\left(u_{II}^h(x_{i+3/2},t)\right) v_l^{(i)}(x_{i+3/2}) + \int_{x^*(t)}^{x_{i+3/2}} f\left(u_{II}^h(x,t)\right) \frac{dv_l^{(i)}(x)}{dx}\, dx \quad (l=0,\ldots,k),$$

$$\tag{2.26}$$

where $\bar{u}_I^{(l)}(t) = \int_{x_{i-3/2}}^{x^*(t)} u_I^h(x,t) v_l^{(i)}(x)\, dx$, $\bar{u}_{II}^{(l)}(t) = \int_{x^*(t)}^{x_{i+3/2}} u_{II}^h(x,t) v_l^{(i)}(x)\, dx$ and $f^*(u(x^*(t),t)) = f(u(x^*(t),t)) - \frac{dx^*(t)}{dt} u(x^*(t),t)$. These ODE systems can be solved by using (2.22). The detailed discussion pertaining to the right-hand sides of (2.25) and (2.26) can be found in [23].

Here we shall emphasize on the WENO type reconstructions for the "troubled cells". As shown in Fig. 2.1, we only present the formulae at the Gaussian points and associated linear weights and omit the smoothness indicators and nonlinear weights equations which are analogous to the regular cell to simplify the main procedures for the WENO type reconstructions.

2.2.1. WENO3 as limiter for application of RKDG2 (WENO3-RKDG2) to interfacial cell

Below, we shall consider the different cases where the "troubled cell" is located and set $x^*(t)$ to be x^*.

Step 2.1.1. Here, I_{i-2} is the "troubled cell". Given the small stencils $S_1 = \{I_{i-3}, I_{i-2}\}$, $S_2 = \{I_{i-2}, \bar{I}_{i-1}\}$ and the bigger stencil $\Gamma = S_1 \cup S_2$, we construct the linear reconstruction polynomials $p_n(x) \in span\{1, (x-x_{i-2})/h\}$ $(n=1,2)$ and a second degree reconstruction polynomial $q(x) \in span\{1, (x-x_{i-2})/h, (x-x_{i-2})^2/h^2\}$, such that:

$$\frac{1}{h} \int_{I_{i+j}} p_1(x)\, dx = u_{i+j}^{(0)}, \quad j = -3, -2, \tag{2.27}$$

$$\frac{1}{h} \int_{I_{i+j}} p_2(x)\, dx = u_{i+j}^{(0)}, \quad j = -2, \tag{2.28}$$

$$\frac{1}{x^* - x_{i-1-\frac{1}{2}}} \int_{\bar{I}_{i+j}} p_2(x)\,dx = \bar{u}_{i+j}^{(0)}, \quad j = -1, \tag{2.29}$$

$$\frac{1}{h} \int_{I_{i+j}} q(x)\,dx = u_{i+j}^{(0)}, \quad j = -3, -2, \tag{2.30}$$

$$\frac{1}{x^* - x_{i-1-\frac{1}{2}}} \int_{\bar{I}_{i+j}} q(x)\,dx = \bar{u}_{i+j}^{(0)}, \quad j = -1. \tag{2.31}$$

At the point $x_{i-2+\frac{\sqrt{3}}{6}}$, we have:

$$p_1(x_{i-2+\frac{\sqrt{3}}{6}}) = \left(-\sqrt{3}u_{i-3}^{(0)} + (6+\sqrt{3})u_{i-2}^{(0)}\right)/6, \tag{2.32}$$

$$p_2(x_{i-2+\frac{\sqrt{3}}{6}}) = \left(2\sqrt{3}\bar{u}_{i-1}^{(0)} + u_{i-2}^{(0)}(15 - 2\sqrt{3} + 6\xi)\right)/(15 + 6\xi). \tag{2.33}$$

At the point $x_{i-2-\frac{\sqrt{3}}{6}}$, we have:

$$p_1(x_{i-2-\frac{\sqrt{3}}{6}}) = \left(\sqrt{3}u_{i-3}^{(0)} + (6-\sqrt{3})u_{i-2}^{(0)}\right)/6, \tag{2.34}$$

$$p_2(x_{i-2-\frac{\sqrt{3}}{6}}) = \left(-2\sqrt{3}\bar{u}_{i-1}^{(0)} + u_{i-2}^{(0)}(15 + 2\sqrt{3} + 6\xi)\right)/(15 + 6\xi). \tag{2.35}$$

Step 2.1.2. Next, we find the combination coefficients. For $x_G = x_{i-2+\frac{\sqrt{3}}{6}}$, the associated linear weights are:

$$\gamma_1 = (4 + 2\xi)/(7 + 2\xi), \qquad \gamma_2 = 3/(7 + 2\xi). \tag{2.36}$$

For $x_G = x_{i-2-\frac{\sqrt{3}}{6}}$, the associated linear weights are:

$$\gamma_1 = (4 + 2\xi)/(7 + 2\xi), \qquad \gamma_2 = 3/(7 + 2\xi). \tag{2.37}$$

Step 2.2.1. Here, $\bar{I}_{i-1}$ is the "troubled cell". Given the small stencils $S_1 = \{I_{i-2}, \bar{I}_{i-1}\}$, $S_2 = \{\bar{I}_{i-1}, \bar{I}_{i+1}\}$ and the bigger stencil $\Gamma = S_1 \cup S_2$, we construct the linear reconstruction polynomials $p_n(x) \in span\{1, (x - \frac{1}{2}(x^* + x_{i-1-\frac{1}{2}}))/(x^* - x_{i-1-\frac{1}{2}})\}$ $(n = 1, 2)$ and a second degree reconstruction polynomial $q(x) \in span\{1, (x - \frac{1}{2}(x^* + x_{i-1-\frac{1}{2}}))/(x^* - x_{i-1-\frac{1}{2}}), (x - \frac{1}{2}(x^* + x_{i-1-\frac{1}{2}}))^2/(x^* - x_{i-1-\frac{1}{2}})^2\}$, such that:

$$\frac{1}{h} \int_{I_{i+j}} p_1(x)\,dx = u_{i+j}^{(0)}, \quad j = -2, \tag{2.38}$$

$$\frac{1}{x^* - x_{i-1-\frac{1}{2}}} \int_{\bar{I}_{i+j}} p_1(x)\,dx = \bar{u}_{i+j}^{(0)}, \quad j = -1, \tag{2.39}$$

$$\frac{1}{x^* - x_{i-1-\frac{1}{2}}} \int_{\bar{I}_{i+j}} p_2(x)\,dx = \bar{u}_{i+j}^{(0)}, \quad j = -1, \tag{2.40}$$

$$\frac{1}{x_{i+1+\frac{1}{2}} - x^*} \int_{\bar{I}_{i+j}} p_2(x)\,dx = \bar{u}_{i+j}^{(0)}, \quad j = 1, \tag{2.41}$$

$$\frac{1}{h} \int_{I_{i+j}} q(x)\,dx = u_{i+j}^{(0)}, \quad j = -2, \tag{2.42}$$

$$\frac{1}{x^* - x_{i-1-\frac{1}{2}}} \int_{\bar{I}_{i+j}} q(x)\,dx = \bar{u}_{i+j}^{(0)}, \quad j = -1, \tag{2.43}$$

$$\frac{1}{x_{i+1+\frac{1}{2}} - x^*} \int_{\bar{I}_{i+j}} q(x)\,dx = \bar{u}_{i+j}^{(0)}, \quad j = 1. \tag{2.44}$$

At the point $\bar{x}_{i-1+\frac{\sqrt{3}}{6}} = \frac{1}{2}(x^* + x_{i-1-\frac{1}{2}}) + \frac{\sqrt{3}}{6}(x^* - x_{i-1-\frac{1}{2}})$, we have:

$$p_1(\bar{x}_{i-1+\frac{\sqrt{3}}{6}}) = \left(-\sqrt{3}u_{i-2}^{(0)}(3+2\xi) + \bar{u}_{i-1}^{(0)}(15+3\sqrt{3}+6\xi+2\sqrt{3}\xi)\right)/(15+6\xi), \tag{2.45}$$

$$p_2(\bar{x}_{i-1+\frac{\sqrt{3}}{6}}) = \left(\sqrt{3}\bar{u}_{i+1}^{(0)}(3+2\xi) + \bar{u}_{i-1}^{(0)}(18-3\sqrt{3}-2\sqrt{3}\xi)\right)/18. \tag{2.46}$$

At the point $\bar{x}_{i-1-\frac{\sqrt{3}}{6}}$, we have:

$$p_1(\bar{x}_{i-1-\frac{\sqrt{3}}{6}}) = \left(\sqrt{3}u_{i-2}^{(0)}(3+2\xi) + \bar{u}_{i-1}^{(0)}(15-3\sqrt{3}+6\xi-2\sqrt{3}\xi)\right)/(15+6\xi), \tag{2.47}$$

$$p_2(\bar{x}_{i-1-\frac{\sqrt{3}}{6}}) = \left(-\sqrt{3}\bar{u}_{i+1}^{(0)}(3+2\xi) + \bar{u}_{i-1}^{(0)}(18+3\sqrt{3}+2\sqrt{3}\xi)\right)/18. \tag{2.48}$$

Step 2.2.2. Next, we find the combination coefficients. For $x_G = \bar{x}_{i-1+\frac{\sqrt{3}}{6}}$, the associated linear weights are:

$$\gamma_1 = (9-2\xi)/16, \qquad \gamma_2 = (7+2\xi)/16. \tag{2.49}$$

For $x_G = \bar{x}_{i-1-\frac{\sqrt{3}}{6}}$, the associated linear weights are:

$$\gamma_1 = (9-2\xi)/16, \qquad \gamma_2 = (7+2\xi)/16. \tag{2.50}$$

Step 2.3.1. Here, $\bar{I}_{i+1}$ is the "troubled cell". Given the small stencils $S_1 = \{\bar{I}_{i-1}, \bar{I}_{i+1}\}$, $S_2 = \{\bar{I}_{i+1}, I_{i+2}\}$ and the bigger stencil $\Gamma = S_1 \cup S_2$, we construct the linear reconstruction polynomials $p_n(x) \in span\{1, (x - \frac{1}{2}(x^* + x_{i+1+\frac{1}{2}}))/(x_{i+1+\frac{1}{2}} - x^*)\}$ $(n = 1, 2)$ and a second degree reconstruction polynomial $q(x) \in span\{1, (x - \frac{1}{2}(x^* + x_{i+1+\frac{1}{2}}))/(x_{i+1+\frac{1}{2}} - x^*), (x - \frac{1}{2}(x^* + x_{i+1+\frac{1}{2}}))^2/(x_{i+1+\frac{1}{2}} - x^*)^2\}$, such that:

$$\frac{1}{x^* - x_{i-1-\frac{1}{2}}} \int_{\bar{I}_{i+j}} p_1(x)\,dx = \bar{u}_{i+j}^{(0)}, \quad j = -1, \tag{2.51}$$

$$\frac{1}{x_{i+1+\frac{1}{2}} - x^*} \int_{\bar{I}_{i+j}} p_1(x)\,dx = \bar{u}_{i+j}^{(0)}, \quad j = 1, \tag{2.52}$$

$$\frac{1}{x_{i+1+\frac{1}{2}} - x^*} \int_{\bar{I}_{i+j}} p_2(x)\,dx = \bar{u}_{i+j}^{(0)}, \quad j = 1, \tag{2.53}$$

$$\frac{1}{h} \int_{I_{i+j}} p_2(x)\,dx = u_{i+j}^{(0)}, \quad j = 2, \tag{2.54}$$

$$\frac{1}{x^* - x_{i-1-\frac{1}{2}}} \int_{\bar{I}_{i+j}} q(x)\,dx = \bar{u}_{i+j}^{(0)}, \quad j = -1, \tag{2.55}$$

$$\frac{1}{x_{i+1+\frac{1}{2}} - x^*} \int_{\bar{I}_{i+j}} q(x)\,dx = \bar{u}_{i+j}^{(0)}, \quad j = 1, \tag{2.56}$$

$$\frac{1}{h} \int_{I_{i+j}} q(x)\,dx = u_{i+j}^{(0)}, \quad j = 2. \tag{2.57}$$

At the point $\bar{x}_{i+1+\frac{\sqrt{3}}{6}} = \frac{1}{2}(x^* + x_{i+1+\frac{1}{2}}) + \frac{\sqrt{3}}{6}(x_{i+1+\frac{1}{2}} - x^*)$, we have:

$$p_1(\bar{x}_{i+1+\frac{\sqrt{3}}{6}}) = \left(-\sqrt{3}\bar{u}_{i-1}^{(0)}(3-2\xi) + \bar{u}_{i+1}^{(0)}(18+3\sqrt{3}-2\sqrt{3}\xi)\right)/18, \tag{2.58}$$

$$p_2(\bar{x}_{i+1+\frac{\sqrt{3}}{6}}) = \left(-\sqrt{3}u_{i+2}^{(0)}(3-2\xi) + \bar{u}_{i+1}^{(0)}(-15+3\sqrt{3}+6\xi-2\sqrt{3}\xi)\right)/(-15+6\xi). \tag{2.59}$$

At the point $\bar{x}_{i+1-\frac{\sqrt{3}}{6}}$, we have:

$$p_1(\bar{x}_{i+1-\frac{\sqrt{3}}{6}}) = \left(\sqrt{3}\bar{u}_{i-1}^{(0)}(3-2\xi) + \bar{u}_{i+1}^{(0)}(18-3\sqrt{3}+2\sqrt{3}\xi)\right)/18, \tag{2.60}$$

$$p_2(\bar{x}_{i+1-\frac{\sqrt{3}}{6}}) = \left(\sqrt{3}u_{i+2}^{(0)}(3-2\xi) + \bar{u}_{i+1}^{(0)}(-15-3\sqrt{3}+6\xi+2\sqrt{3}\xi)\right)/(-15+6\xi). \tag{2.61}$$

Step 2.3.2. Next, we find the combination coefficients. For $x_G = \bar{x}_{i+1+\frac{\sqrt{3}}{6}}$, the associated linear weights are:

$$\gamma_1 = (7-2\xi)/16, \qquad \gamma_2 = (9+2\xi)/16. \tag{2.62}$$

For $x_G = \bar{x}_{i+1-\frac{\sqrt{3}}{6}}$, the associated linear weights are:

$$\gamma_1 = (7-2\xi)/16, \qquad \gamma_2 = (9+2\xi)/16. \tag{2.63}$$

Step 2.4.1. Here, I_{i+2} is the "troubled cell". Given the small stencils $S_1 = \{\bar{I}_{i+1}, I_{i+2}\}$, $S_2 = \{I_{i+2}, I_{i+3}\}$ and the bigger stencil $\Gamma = S_1 \cup S_2$, we construct the linear reconstruction polynomials $p_n(x) \in span\{1, (x-x_{i+2})/h\}$ ($n = 1, 2$) and a second degree reconstruction polynomial $q(x) \in span\{1, (x-x_{i+2})/h, (x-x_{i+2})^2/h^2\}$, such that:

$$\frac{1}{x_{i+1+\frac{1}{2}} - x^*} \int_{\bar{I}_{i+j}} p_1(x)\,dx = \bar{u}_{i+j}^{(0)}, \quad j = 1, \tag{2.64}$$

$$\frac{1}{h} \int_{I_{i+j}} p_1(x)\,dx = u_{i+j}^{(0)}, \quad j = 2, \tag{2.65}$$

$$\frac{1}{h} \int_{I_{i+j}} p_2(x)\,dx = u_{i+j}^{(0)}, \quad j = 2, 3, \tag{2.66}$$

$$\frac{1}{x_{i+1+\frac{1}{2}} - x^*} \int_{\bar{I}_{i+j}} q(x)\,dx = \bar{u}_{i+j}^{(0)}, \quad j = 1, \tag{2.67}$$

$$\frac{1}{h} \int_{I_{i+j}} q(x)\,dx = u_{i+j}^{(0)}, \quad j = 2, 3. \tag{2.68}$$

At the point $x_{i+2+\frac{\sqrt{3}}{6}}$, we have:

$$p_1(x_{i+2+\frac{\sqrt{3}}{6}}) = \left(2\sqrt{3}\bar{u}_{i+1}^{(0)} + u_{i+2}^{(0)}(-15-2\sqrt{3}+6\xi)\right)/(-15+6\xi), \tag{2.69}$$

$$p_2(x_{i+2+\frac{\sqrt{3}}{6}}) = \left((6-\sqrt{3})u_{i+2}^{(0)} + \sqrt{3}u_{i+3}^{(0)}\right)/6. \tag{2.70}$$

At the point $x_{i+2-\frac{\sqrt{3}}{6}}$, we have:

$$p_1(x_{i+2-\frac{\sqrt{3}}{6}}) = \left(-2\sqrt{3}\bar{u}_{i+1}^{(0)} + u_{i+2}^{(0)}(-15+2\sqrt{3}+6\xi)\right)/(-15+6\xi), \tag{2.71}$$

$$p_2(x_{i+2-\frac{\sqrt{3}}{6}}) = \left((6+\sqrt{3})u_{i+2}^{(0)} - \sqrt{3}u_{i+3}^{(0)}\right)/6. \tag{2.72}$$

Step 2.4.2. Next, we find the combination coefficients. For $x_G = x_{i+2+\frac{\sqrt{3}}{6}}$, the associated linear weights are:

$$\gamma_1 = 3/(7-2\xi), \qquad \gamma_2 = (4-2\xi)/(7-2\xi). \tag{2.73}$$

For $x_G = x_{i+2-\frac{\sqrt{3}}{6}}$, the associated linear weights are:

$$\gamma_1 = 3/(7-2\xi), \qquad \gamma_2 = (4-2\xi)/(7-2\xi). \tag{2.74}$$

Remark. In this paper, it is the intent to have conservative treatment of the material interface and maintain the numerical schemes' high-order of accuracy near the interface. For this purpose, we shall define the Riemann problem at the material interface, solve for the problem and get the densities (ρ_{IL} and ρ_{IR}), velocity (u_I) and pressure (p_I). Then we employ the isobaric fix [13] to get the variables of another side cells of the material interface for the WENO or HWENO reconstructions, respectively.

Provided in Appendices A–D is the third-order $k = 2$ case for reconstruction of the first and second moments $u_i^{(1)}$ and $u_i^{(2)}$ applicable to the "troubled cells" I_i via WENO5 or HWENO5.

Table 3.1

1D Euler equations. $\rho(x,0) = 1 + 0.2\sin(\pi x)$, $v(x,0) = 1$, $p(x,0) = 1$. Periodic boundary conditions. WENO3-RKDG2 scheme; WENO5-RKDG3 scheme; HWENO5-RKDG3 scheme. $t = 2$. L^1 and L^∞ errors.

| Cells	WENO3-RKDG2 scheme				WENO5-RKDG3 scheme				WENO5-RKDG3 scheme			
	L^1 error	Order	L^∞ error	Order	L^1 error	Order	L^∞ error	Order	L^1 error	Order	L^∞ error	Order
10	5.27E−3		1.76E−2		2.96E−4		3.28E−3		2.96E−4		3.28E−3	
20	8.72E−4	2.60	2.80E−3	2.65	2.85E−5	3.38	4.67E−4	2.81	2.85E−5	3.38	4.67E−4	2.81
40	1.81E−4	2.26	7.45E−4	1.91	2.83E−6	3.33	5.99E−5	2.96	2.83E−6	3.33	5.99E−5	2.96
80	4.23E−5	2.10	1.96E−4	1.92	3.05E−7	3.21	7.51E−6	2.99	3.05E−7	3.21	7.51E−6	2.99
160	1.02E−5	2.04	5.03E−5	1.97	3.50E−8	3.12	9.39E−7	3.00	3.50E−8	3.12	9.39E−7	3.00
320	2.53E−6	2.02	1.27E−5	1.98	4.18E−9	3.07	1.17E−7	3.00	4.18E−9	3.07	1.17E−7	3.00
640	6.30E−7	2.01	3.19E−6	1.99	5.11E−10	3.03	1.46E−8	3.00	5.11E−10	3.03	1.46E−8	3.00
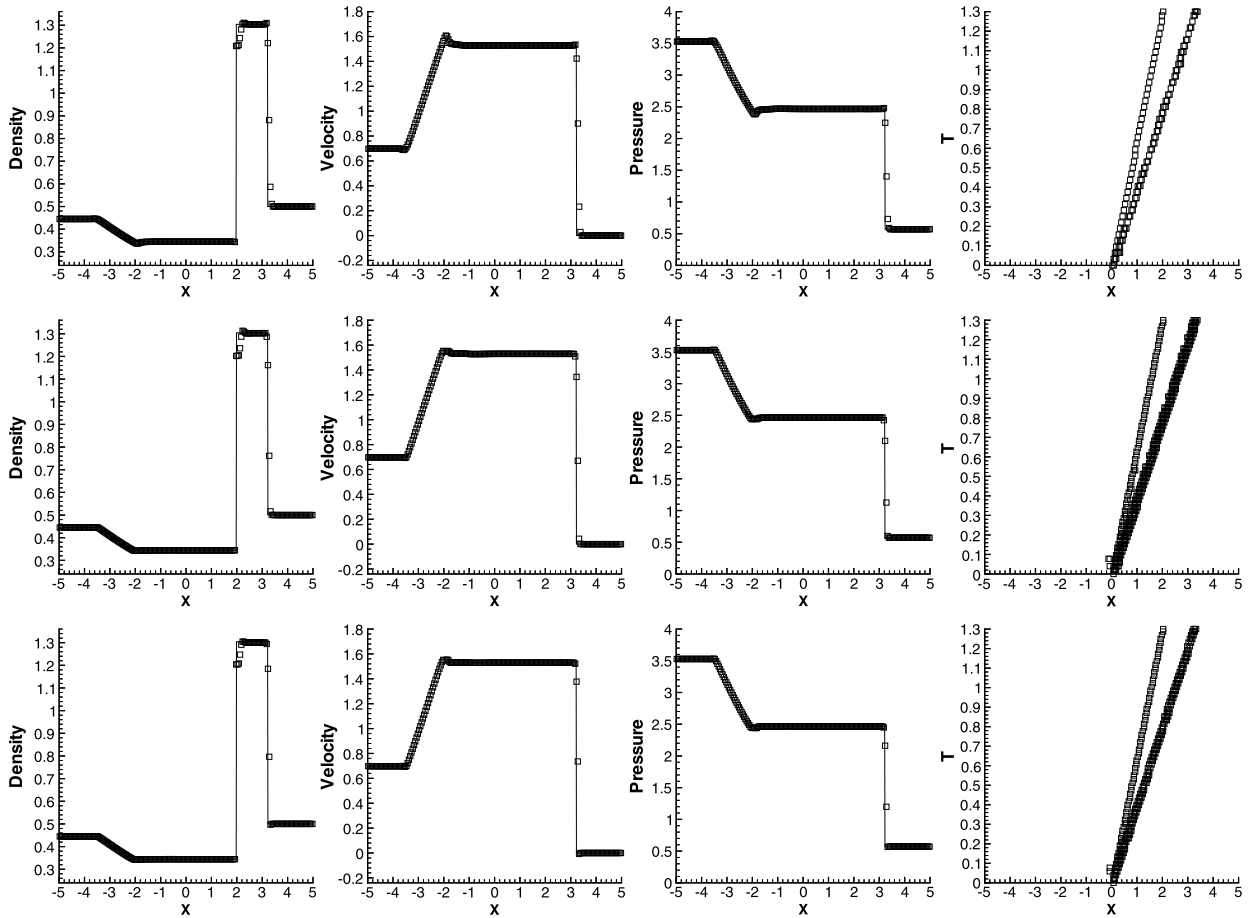
Fig. 3.1. On Example 3.2. Left to right: density; velocity; pressure; time history of the "troubled cells". $t = 1.3$. Top to bottom: WENO3-RKDG2; WENO5-RKDG3; HWENO5-RKDG3. Line: exact solution; squares: numerical solution with 200 cells.

3. Numerical tests

In this section, we present the results of numerical tests for the schemes described in the previous section for both single-medium and multi-medium flows (which include gas–gas and gas–water cases). In this paper, we choose the CFL number to be 0.3 for WENO3-RKDG2 ($k = 1$) and 0.18 for WENO5-RKDG3 ($k = 2$) and HWENO5-RKDG3 ($k = 2$), respectively.

Example 3.1. We solve the one-dimensional nonlinear Euler equations (2.1). The initial condition is set to be $\rho(x,0) = 1 + 0.2\sin(\pi x)$, $v(x,0) = 1$, $p(x,0) = 1$, $x \in [0, 2]$ with periodic boundary conditions. The exact solution is $\rho(x,t) = 1 + 0.2\sin(\pi(x-t))$, $v(x,t) = 1$, $p(x,t) = 1$. The initial artificial interface is set at $x^*(0) = 1$. We compute the solution up to $t = 2$. The errors and numerical orders of accuracy are shown in Table 3.1. It is clear that the three schemes have achieved their designed order of accuracy. We have used the KXRCF indicator to identify the "troubled cells". However, for this test
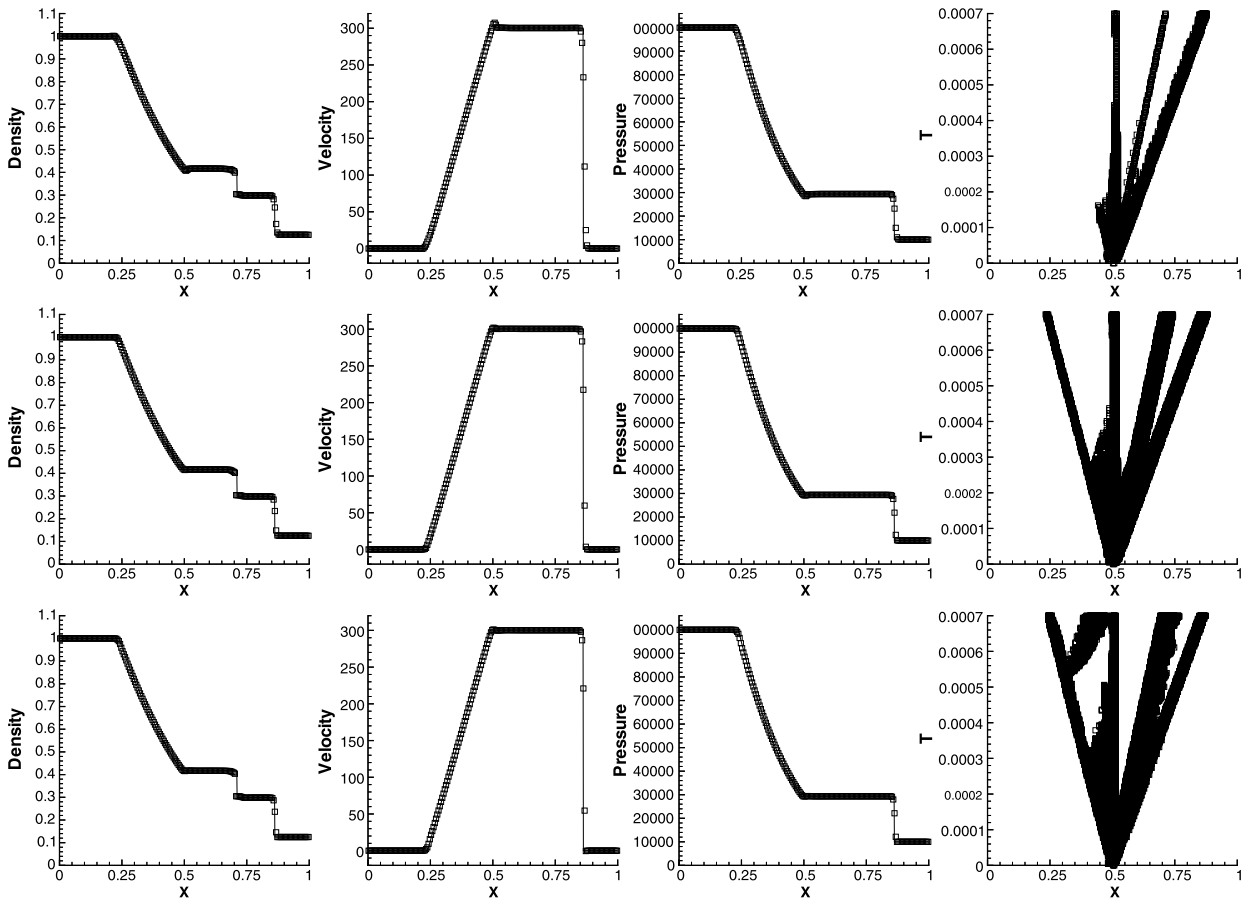
Fig. 3.2. On Example 3.3. Left to right: density; velocity; pressure; time history of the "troubled cells". $t = 0.0007$. Top to bottom: WENO3-RKDG2; WENO5-RKDG3; HWENO5-RKDG3. Line: exact solution; squares: numerical solution with 200 cells.

case, in the determination of the super-convergence property, the KXRCF indicator showed that no "troubled cell" is present. As such, the results shown here are the same as those obtained employing DG without limiter for all the norms.

Example 3.2. We solve the Euler equations (2.1). We use the following Riemann initial condition for the Lax problem:

$$(\rho, v, p, \gamma)^T = \begin{cases} (0.445, 0.698, 3.528, 1.4)^T & x \leqslant 0, \\ (0.5, 0, 0.571, 1.4)^T & x > 0. \end{cases} \tag{3.1}$$

The computational domain is $[-5, 5]$ with open boundary conditions. The computed density, velocity and pressure are plotted at $t = 1.3$ against the exact solution. The solutions using 200 cells and the time history of the "troubled cells" are shown in Fig. 3.1. The initial material interface is set at $x^*(0) = 0$. We can see that the resolutions of the contact discontinuity by the RKDG methods are good for both $k = 1$ and $k = 2$ using WENO or HWENO reconstructions as limiters. And the material interface is resolved properly too.

Below, we present the results of numerical tests for the gas–gas and gas–water flows by the WENO3-RKDG2, WENO5-RKDG3 and HWENO5-RKDG3 schemes described in Section 2. In these tests, 200 cells are used. The units for the density, velocity, pressure, length and time are kg/m^3, m/s, Pa, m and s, respectively.

Example 3.3. This is an air–helium shock tube problem taken from [13], with the initial conditions as:

$$(\rho, v, p, \gamma)^T = \begin{cases} (1, 0, 10^5, 1.4)^T & x \leqslant 0.5, \\ (0.125, 0, 10^4, 1.2)^T & x > 0.5. \end{cases} \tag{3.2}$$

The computational domain is $[0, 1]$ with open boundary conditions. The computed density, velocity and pressure are plotted at $t = 0.0007$ against the exact solutions and the time history of the "troubled cells" in Fig. 3.2. The initial material interface is set at $x^*(0) = 0.5$. The location of the material interface is captured correctly by the WENO3-RKDG2, WENO5-RKDG3 and HWENO5-RKDG3 schemes and are very comparable to the analysis.
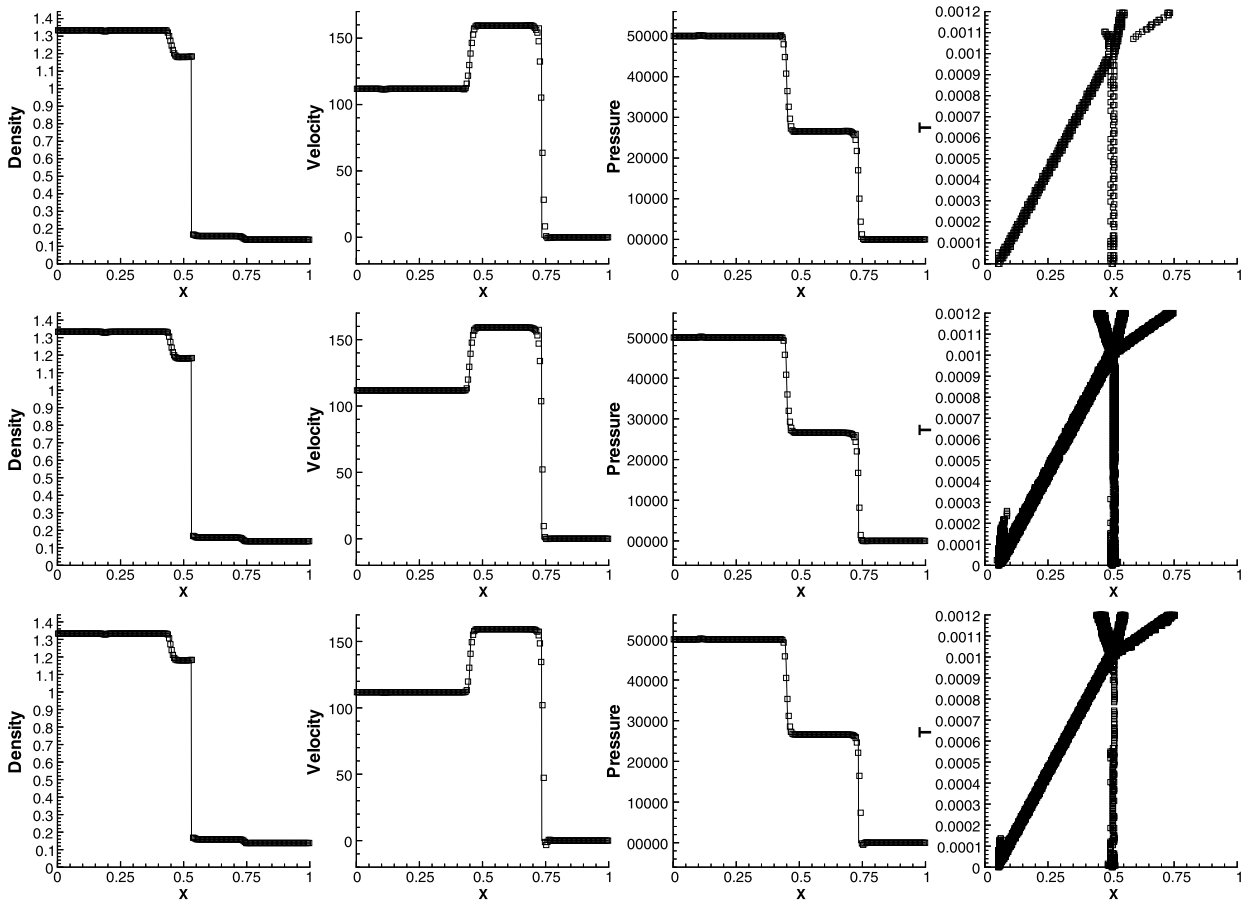
Fig. 3.3. On Example 3.4. Left to right: density; velocity; pressure; time history of the "troubled cells". $t = 0.0012$. Top to bottom: WENO3-RKDG2; WENO5-RKDG3; HWENO5-RKDG3. Line: exact solution; squares: numerical solution with 200 cells.

Example 3.4. This is a problem of a shock wave refracting at an air–helium interface with a reflected rarefaction wave [13]. The flow initial conditions are:

$$(\rho, v, p, \gamma)^T = \begin{cases} (1.3333, 0.3535\sqrt{10^5}, 1.5 \times 10^5, 1.4)^T & x \leqslant 0.05, \\ (1, 0, 10^5, 1.4)^T & 0.05 < x \leqslant 0.5, \\ (0.1379, 0, 10^5, 5/3)^T & x > 0.5. \end{cases} \qquad (3.3)$$

The computational domain is $[0, 1]$ with open boundary conditions. The computed density, velocity and pressure are plotted at $t = 0.0012$ against the exact solutions and the time history of the "troubled cells" in Fig. 3.3. The strength of the shock is $p_L/p_R = 1.5$ and the initial material interface is set at $x^*(0) = 0.5$. The location of the material interface is captured correctly by the WENO3-RKDG2, WENO5-RKDG3 and HWENO5-RKDG3 schemes. There is good concurrence of results with the analysis.

Example 3.5. We consider the Euler equations (2.1) with the following Riemann initial conditions:

$$(\rho, v, p, \gamma)^T = \begin{cases} (1.3333, 0.3535\sqrt{10^5}, 1.5 \times 10^5, 1.4)^T & x \leqslant 0.05, \\ (1, 0, 10^5, 1.4)^T & 0.05 < x \leqslant 0.5, \\ (3.1538, 0, 10^5, 1.249)^T & x > 0.5. \end{cases} \qquad (3.4)$$

The computational domain is $[0, 1]$ with open boundary conditions. The computed density, velocity and pressure are plotted at $t = 0.0017$ against the exact solutions and the time history of the "troubled cells" in Fig. 3.4. The initial material interface is set at $x^*(0) = 0.5$. The location of the material interface is captured correctly. The computed results are oscillatory free at the neighborhood of the interface for the density, velocity and pressure.

Example 3.6. We define the strength of right shock wave to be $p_L/p_R = 15$. So in this case, we compute for the Riemann problems with the following initial conditions:
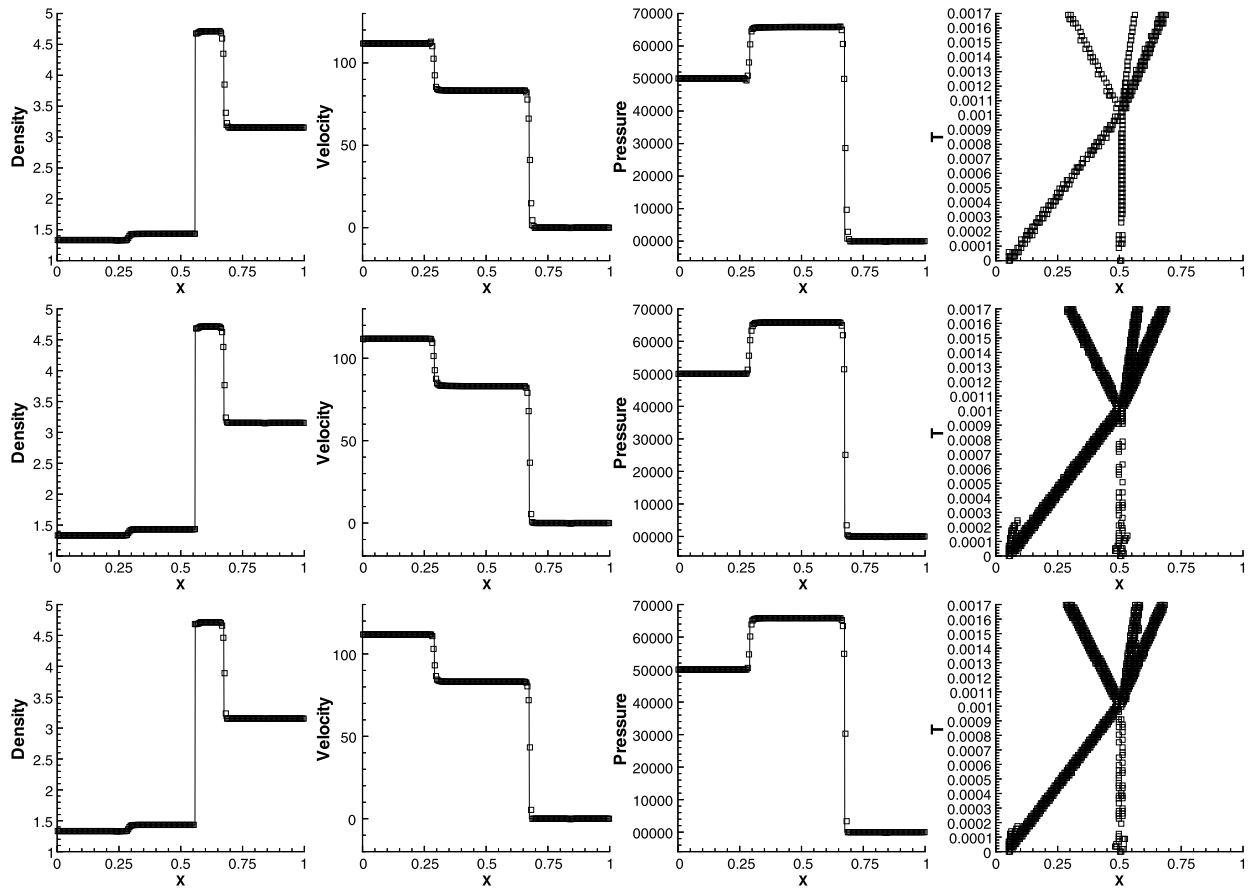
Fig. 3.4. On Example 3.5. Left to right: density; velocity; pressure; time history of the "troubled cells". $t = 0.0017$. Top to bottom: WENO3-RKDG2; WENO5-RKDG3; HWENO5-RKDG3. Line: exact solution; squares: numerical solution with 200 cells.

$$(\rho, v, p, \gamma)^T = \begin{cases} (4.3333, 3.2817\sqrt{10^5}, 1.5 \times 10^6, 1.4)^T & x \leqslant 0.05, \\ (1, 0, 10^5, 1.4)^T & 0.05 < x \leqslant 0.5, \\ (3.1538, 0, 10^5, 1.249)^T & x > 0.5. \end{cases} \qquad (3.5)$$

The computational domain is $[0, 1]$ with open boundary conditions. The computed density, velocity and pressure are plotted at $t = 0.0007$ against the exact solutions and the time history of the "troubled cells" in Fig. 3.5. The initial material interface is set at $x^*(0) = 0.5$. We can also see that the location of the material interface is captured correctly. And there is also a local but limited hump lying in the smooth region, similar to that found in [13,23].

Example 3.7. This is a gas–water shock tube problem with very high pressure in the gaseous medium. The initial conditions are:

$$(\rho, v, p, \gamma)^T = \begin{cases} (1270, 0, 8 \times 10^8, 1.4)^T & x \leqslant 0.5, \\ (1000, 0, 10^5, 7.15)^T & x > 0.5. \end{cases} \qquad (3.6)$$

The computational domain is $[0, 1]$ with open boundary conditions. The computed density, velocity and pressure are plotted at $t = 0.00016$ against the exact solutions and the time history of the "troubled cells" in Fig. 3.6. The initial material interface is set at $x^*(0) = 0.5$. The location of the gas–water interface is captured correctly by all the WENO3-RKDG2, WENO5-RKDG3 and HWENO5-RKDG3 schemes.

Example 3.8. We greatly increase the energy of the explosive gaseous medium in the previous example with the initial conditions set as:

$$(\rho, v, p, \gamma)^T = \begin{cases} (1630, 0, 7.81 \times 10^9, 1.4)^T & x \leqslant 0.5, \\ (1000, 0, 10^5, 7.15)^T & x > 0.5. \end{cases} \qquad (3.7)$$

The computational domain is $[0, 1]$ with open boundary conditions. The computed density, velocity and pressure are plotted at $t = 0.0001$ against the exact solutions and the time history of the "troubled cells" in Fig. 3.7. The initial material interface
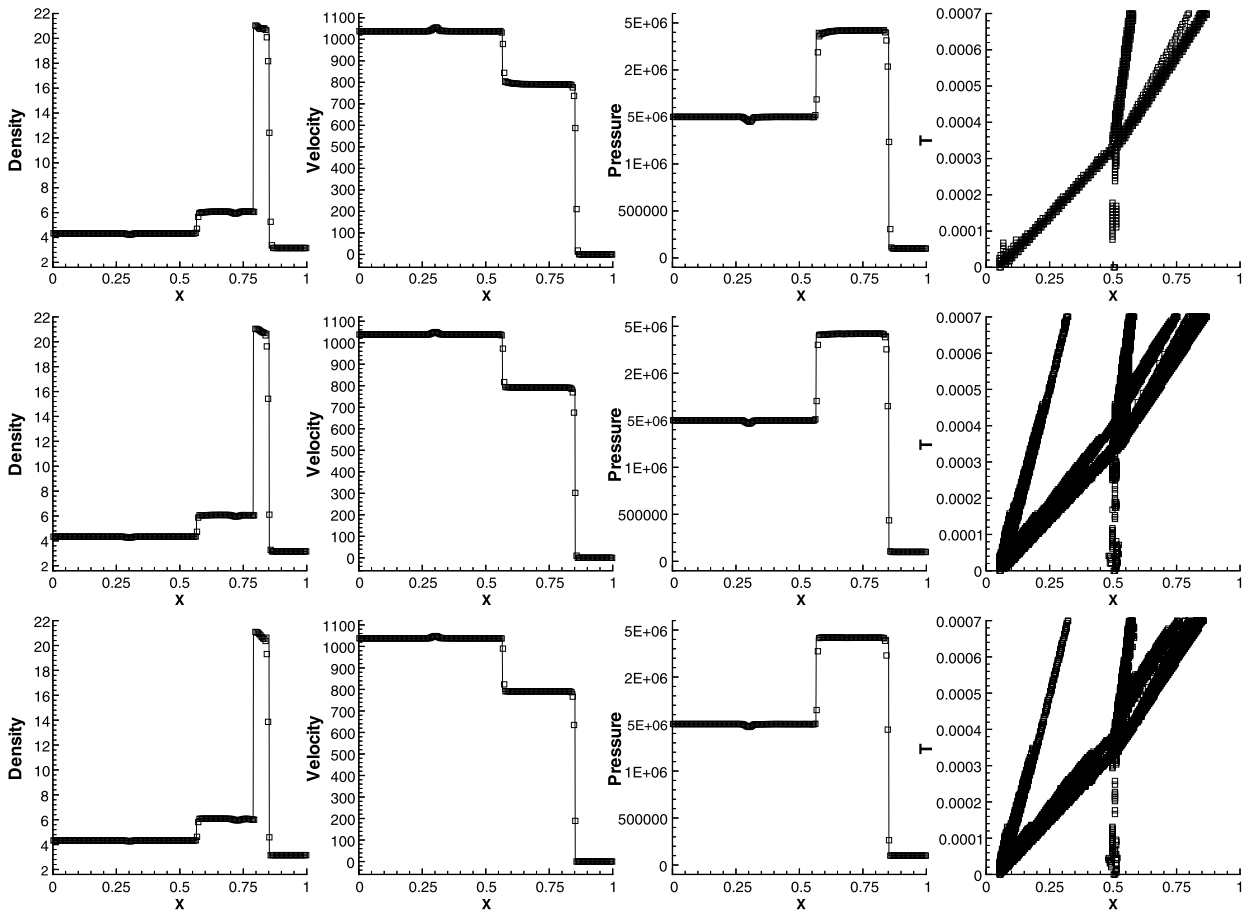
Fig. 3.5. On Example 3.6. Left to right: density; velocity; pressure; time history of the "troubled cells". $t = 0.0007$. Top to bottom: WENO3-RKDG2; WENO5-RKDG3; HWENO5-RKDG3. Line: exact solution; squares: numerical solution with 200 cells.

is set at $x^*(0) = 0.5$. We can see that the location of the material interface is captured correctly by the WENO3-RKDG2, WENO5-RKDG3 and HWENO5-RKDG3 schemes. Further, it is clear that there is much better agreement of the computed velocity and pressure with the analysis as compared to the previous work found in [23].

4. Concluding remarks

We have developed the WENO and HWENO reconstructions as limiters for the RKDG methods to solve for the multi-medium flow in one dimension. The idea is to first identify the "troubled cells" by using a KXRCF indicator, then reconstruct the polynomial solutions inside the "troubled cells" by WENO or HWENO reconstructions using the cell averages or derivative averages of neighboring cells, while maintaining the original cell averages of the "troubled cells" with the proposed conservative treatment of the moving material interface [23]. Compared to [23], in their approach employing the TVB limiter to identify the "troubled cell" and reconstruction depends to some extent on the proper M selected and use of the Lax-Friedrichs flux which has larger numerical viscosity, our present employment of the KXRCF (with super-convergence property) to identify the "troubled cell" and use of WENO/HWENO reconstructions with the HLLC flux are deemed much more straightforward obviating the need to select a viable M value and possibly more accurate. Extensive numerical results for both gas–gas and gas–water flows in one dimension are provided to show that the methods are stable, accurate, and robust subject to a wide range of initial conditions. The proposed methods have been found to be able to provide an accurate and sharp real interface location and still with reasonable solution for the whole domain with very limited oscillations in the interfacial regions.

Appendix

In Appendices A, B, C and D, we reconstruct the first and second moments $u_i^{(1)}$ and $u_i^{(2)}$ for the "troubled cells" I_i by using the WENO5 or HWENO5 to regular cell and interfacial cell in details. The procedures are provided for the "troubled cells" at different locations.
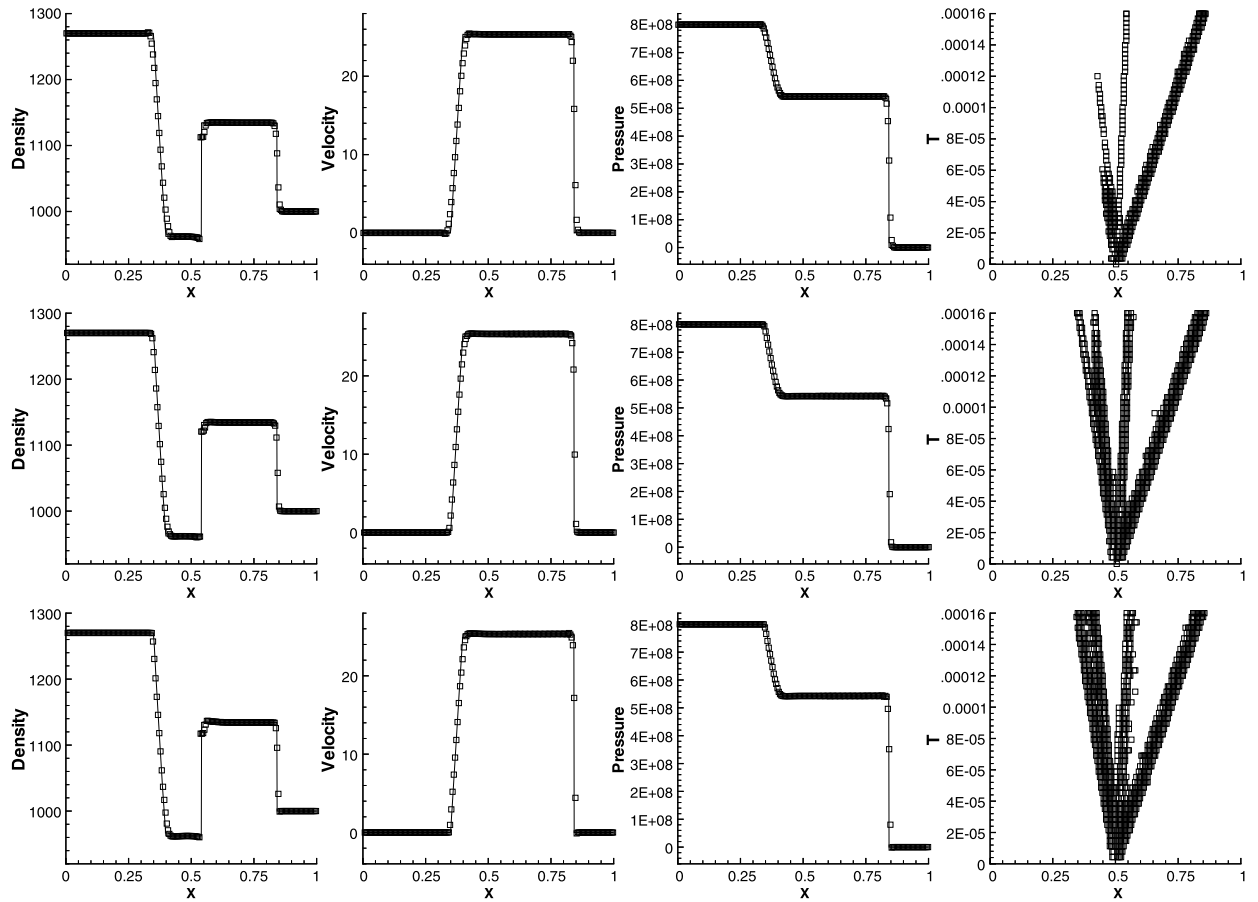
Fig. 3.6. On Example 3.7. Left to right: density; velocity; pressure; time history of the "troubled cells". $t = 0.00016$. Top to bottom: WENO3-RKDG2; WENO5-RKDG3; HWENO5-RKDG3. Line: exact solution; squares: numerical solution with 200 cells.

Appendix A. WENO5 as limiter for application of RKDG3 (WENO5-RKDG3) to regular cell

Step A.1. Given the small stencils $S_1 = \{I_{i-2}, I_{i-1}, I_i\}$, $S_2 = \{I_{i-1}, I_i, I_{i+1}\}$, $S_3 = \{I_i, I_{i+1}, I_{i+2}\}$ and the bigger stencil $\Gamma = S_1 \cup S_2 \cup S_3$, we construct the quadratic reconstruction polynomials $p_n(x) \in span\{1, (x-x_i)/h, (x-x_i)^2/h^2\}$ $(n = 1, 2, 3)$ and a fourth degree reconstruction polynomial $q(x) \in span\{1, (x-x_i)/h, (x-x_i)^2/h^2, (x-x_i)^3/h^3, (x-x_i)^4/h^4\}$, such that:

$$\frac{1}{h} \int_{I_{i+j}} p_1(x)\,dx = u_{i+j}^{(0)}, \quad j = -2, -1, 0, \tag{A.1}$$

$$\frac{1}{h} \int_{I_{i+j}} p_2(x)\,dx = u_{i+j}^{(0)}, \quad j = -1, 0, 1, \tag{A.2}$$

$$\frac{1}{h} \int_{I_{i+j}} p_3(x)\,dx = u_{i+j}^{(0)}, \quad j = 0, 1, 2, \tag{A.3}$$

$$\frac{1}{h} \int_{I_{i+j}} q(x)\,dx = u_{i+j}^{(0)}, \quad j = -2, -1, 0, 1, 2. \tag{A.4}$$

At the point $x_{i+\frac{\sqrt{3}}{6}}$, we have:

$$p_1(x_{i+\frac{\sqrt{3}}{6}}) = \left(u_{i-2}^{(0)} - 4u_{i-1}^{(0)}\right)\sqrt{3}/12 + u_i^{(0)}(1 + \sqrt{3}/4), \tag{A.5}$$

$$p_2(x_{i+\frac{\sqrt{3}}{6}}) = -u_{i-1}^{(0)}\sqrt{3}/12 + u_i^{(0)} + u_{i+1}^{(0)}\sqrt{3}/12, \tag{A.6}$$
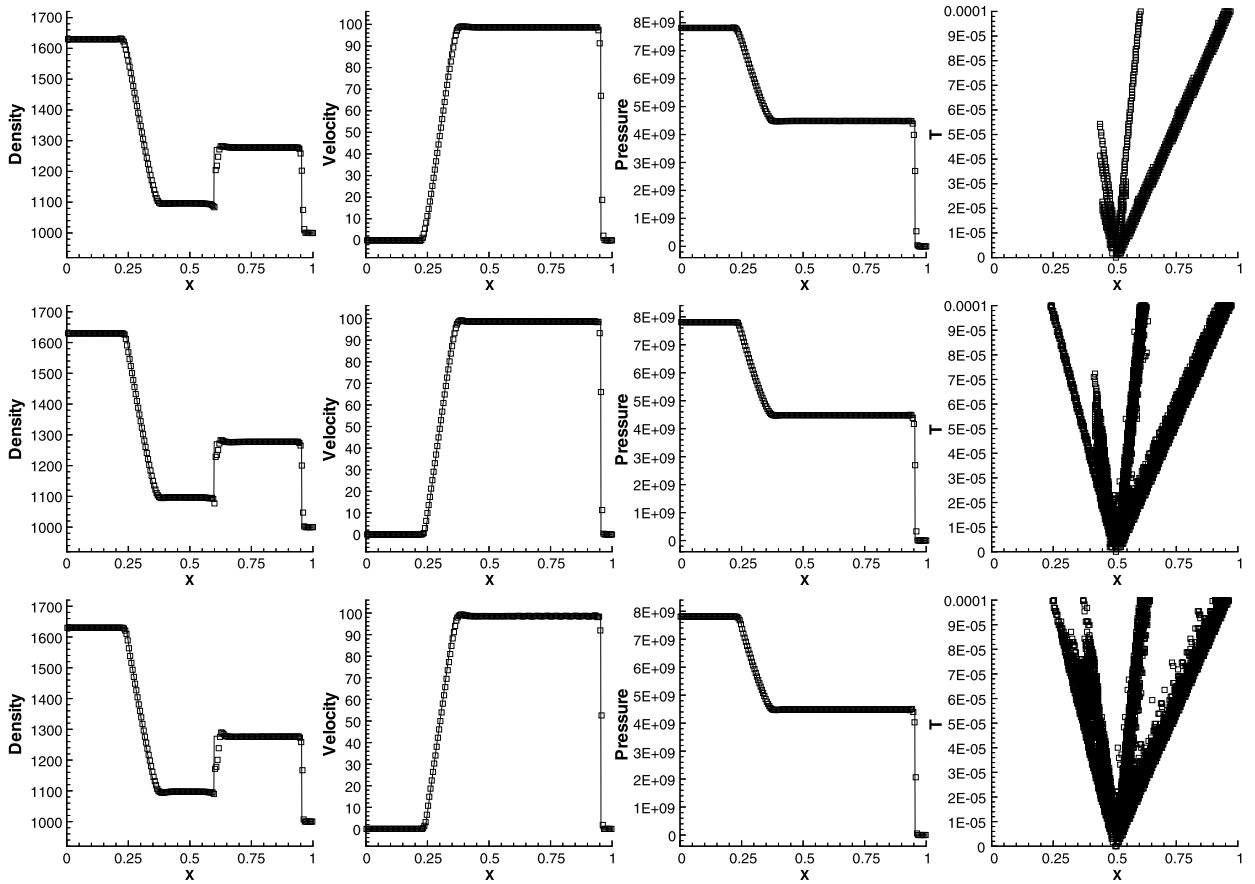
Fig. 3.7. On Example 3.8. Left to right: density; velocity; pressure; time history of the "troubled cells". $t = 0.0001$. Top to bottom: WENO3-RKDG2; WENO5-RKDG3; HWENO5-RKDG3. Line: exact solution; squares: numerical solution with 200 cells.

$$p_3(x_{i+\frac{\sqrt{3}}{6}}) = u_i^{(0)}(1 - \sqrt{3}/4) + \big(4u_{i+1}^{(0)} - u_{i+2}^{(0)}\big)\sqrt{3}/12. \tag{A.7}$$

At the point $x_{i-\frac{\sqrt{3}}{6}}$, we have:

$$p_1(x_{i-\frac{\sqrt{3}}{6}}) = \big(4u_{i-1}^{(0)} - u_{i-2}^{(0)}\big)\sqrt{3}/12 + u_i^{(0)}(1 - \sqrt{3}/4), \tag{A.8}$$

$$p_2(x_{i-\frac{\sqrt{3}}{6}}) = u_{i-1}^{(0)}\sqrt{3}/12 + u_i^{(0)} - u_{i+1}^{(0)}\sqrt{3}/12, \tag{A.9}$$

$$p_3(x_{i-\frac{\sqrt{3}}{6}}) = (1 + \sqrt{3}/4)u_i^{(0)} + \big(-4u_{i+1}^{(0)} + u_{i+2}^{(0)}\big)\sqrt{3}/12. \tag{A.10}$$

Step A.2. We find the combination coefficients, also called linear weights, denoted by $\gamma_1, \gamma_2, \gamma_3$, which satisfy: $q(x_G) = \sum_{j=1}^{3} \gamma_j p_j(x_G)$. For $x_G = x_{i+\frac{\sqrt{3}}{6}}$, the associated linear weights are:

$$\gamma_1 = (210 - \sqrt{3})/1080, \qquad \gamma_2 = 11/18, \qquad \gamma_3 = (210 + \sqrt{3})/1080. \tag{A.11}$$

For $x_G = x_{i-\frac{\sqrt{3}}{6}}$, the associated linear weights are:

$$\gamma_1 = (210 + \sqrt{3})/1080, \qquad \gamma_2 = 11/18, \qquad \gamma_3 = (210 - \sqrt{3})/1080. \tag{A.12}$$

Step A.3. We compute the smoothness indicators β_n $(n = 1, 2, 3)$ for stencils S_n $(n = 1, 2, 3)$:

$$\beta_n = \sum_{\alpha=1}^{2} \int_{I_i} h^{2\alpha-1} \left(\frac{d^\alpha p_n(x)}{dx^\alpha} \right)^2 dx \quad (n = 1, 2, 3). \tag{A.13}$$

Step A.4. We compute the nonlinear weights based on the smoothness indicators:

$$\omega_n = \frac{\bar{\omega}_n}{\sum_{l=1}^{3} \bar{\omega}_l}, \qquad \bar{\omega}_n = \frac{\gamma_n}{\sum_{l=1}^{3}(10^{-6} + \beta_l)^2} \quad (n = 1, 2, 3). \tag{A.14}$$

Then the final WENO5 approximations are given by:

$$u(x_G, t) \approx \sum_{n=1}^{3} \omega_n p_n(x_G). \tag{A.15}$$

Step A.5. We obtain the reconstructed moments based on the reconstructed point values $u(x_G, t)$ at the Gaussian quadrature points x_G and a numerical integration:

$$u_i^{(l)}(t) \approx \frac{1}{\sum_G \sigma_G (v_l^{(i)}(x_G))^2} \sum_G \sigma_G u(x_G, t) v_l^{(i)}(x_G) \quad (l = 1, 2). \tag{A.16}$$

Here σ_G is the Gaussian quadrature weight for the point x_G. The polynomial solution in this cell I_i is then obtained by $u^h(x, t) = \sum_{l=0}^{2} u_i^{(l)}(t) v_l^{(i)}(x)$, for $x \in I_i$ with these reconstructed moments $u_i^{(l)}(t)$ $(l = 1, 2)$ and the original cell average $u_i^{(0)}(t)$.

Appendix B. HWENO5 as limiter for application of RKDG3 (HWENO5-RKDG3) to regular cell

Step B.1. Given the small stencils $S_1 = \{I_{i-1}, I_i\}$, $S_2 = \{I_i, I_{i+1}\}$, $S_3 = \{I_{i-1}, I_i, I_{i+1}\}$ and the bigger stencil $\Gamma = S_1 \cup S_2 \cup S_3$, we construct the quadratic reconstruction polynomials $p_n(x) \in span\{1, (x - x_i)/h, (x - x_i)^2/h^2\}$ $(n = 1, 2, 3)$ and a fourth degree reconstruction polynomial $q(x) \in span\{1, (x - x_i)/h, (x - x_i)^2/h^2, (x - x_i)^3/h^3, (x - x_i)^4/h^4\}$ such that:

$$\frac{1}{h} \int_{I_{i+j}} p_1(x)\,dx = u_{i+j}^{(0)}, \quad j = -1, 0, \tag{B.17}$$

$$\frac{1}{\int_{I_{i+j}}(v_1^{(i+j)}(x))^2\,dx} \int_{I_{i+j}} p_1(x) v_1^{(i+j)}(x)\,dx = u_{i+j}^{(1)}, \quad j = -1, \tag{B.18}$$

$$\frac{1}{h} \int_{I_{i+j}} p_2(x)\,dx = u_{i+j}^{(0)}, \quad j = 0, 1, \tag{B.19}$$

$$\frac{1}{\int_{I_{i+j}}(v_1^{(i+j)}(x))^2\,dx} \int_{I_{i+j}} p_2(x) v_1^{(i+j)}(x)\,dx = u_{i+j}^{(1)}, \quad j = 1, \tag{B.20}$$

$$\frac{1}{h} \int_{I_{i+j}} p_3(x)\,dx = u_{i+j}^{(0)}, \quad j = -1, 0, 1, \tag{B.21}$$

$$\frac{1}{h} \int_{I_{i+j}} q(x)\,dx = u_{i+j}^{(0)}, \quad j = -1, 0, 1, \tag{B.22}$$

$$\frac{1}{\int_{I_{i+j}}(v_1^{(i+j)}(x))^2\,dx} \int_{I_{i+j}} q(x) v_1^{(i+j)}(x)\,dx = u_{i+j}^{(1)}, \quad j = -1, 1. \tag{B.23}$$

At the point $x_{i+\frac{\sqrt{3}}{6}}$, we have:

$$p_1(x_{i+\frac{\sqrt{3}}{6}}) = -u_{i-1}^{(0)}\sqrt{3}/3 + u_i^{(0)}(1 + \sqrt{3}/3) - u_{i-1}^{(1)}\sqrt{3}/6, \tag{B.24}$$

$$p_2(x_{i+\frac{\sqrt{3}}{6}}) = u_i^{(0)}(1 - \sqrt{3}/3) + (2u_{i+1}^{(0)} - u_{i+1}^{(1)})\sqrt{3}/6, \tag{B.25}$$

$$p_3(x_{i+\frac{\sqrt{3}}{6}}) = -u_{i-1}^{(0)}\sqrt{3}/12 + u_i^{(0)} + u_{i+1}^{(0)}\sqrt{3}/12. \tag{B.26}$$

At the point $x_{i-\frac{\sqrt{3}}{6}}$, we have:

$$p_1(x_{i-\frac{\sqrt{3}}{6}}) = u_{i-1}^{(0)}\sqrt{3}/3 + u_i^{(0)}(1 - \sqrt{3}/3) + u_{i-1}^{(1)}\sqrt{3}/6, \tag{B.27}$$

$$p_2(x_{i-\frac{\sqrt{3}}{6}}) = u_i^{(0)}(1 + \sqrt{3}/3) + (-2u_{i+1}^{(0)} + u_{i+1}^{(1)})\sqrt{3}/6, \tag{B.28}$$

$$p_3(x_{i-\frac{\sqrt{3}}{6}}) = u_{i-1}^{(0)}\sqrt{3}/12 + u_i^{(0)} - u_{i+1}^{(0)}\sqrt{3}/12. \tag{B.29}$$

Step B.2. We find the combination coefficients, also called linear weights, denoted by $\gamma_1, \gamma_2, \gamma_3$, which satisfy: $q(x_G) = \sum_{j=1}^{3} \gamma_j p_j(x_G)$. For $x_G = x_{i+\frac{\sqrt{3}}{6}}$, the associated linear weights are:

$$\gamma_1 = 35/114 - 1/(96\sqrt{3}), \qquad \gamma_2 = 35/114 + 1/(96\sqrt{3}), \qquad \gamma_3 = 22/57. \tag{B.30}$$

For $x_G = x_{i-\frac{\sqrt{3}}{6}}$, the associated linear weights are:

$$\gamma_1 = 35/114 + 1/(96\sqrt{3}), \qquad \gamma_2 = 35/114 - 1/(96\sqrt{3}), \qquad \gamma_3 = 22/57. \tag{B.31}$$

The latter steps are similar to the previous section and hence omitted.

Appendix C. WENO5 as limiter for application of RKDG3 (WENO5-RKDG3) to interfacial cell

Step C.1.1. Here, I_{i-3} is the "troubled cell". Given the small stencils $S_1 = \{I_{i-5}, I_{i-4}, I_{i-3}\}$, $S_2 = \{I_{i-4}, I_{i-3}, I_{i-2}\}$, $S_3 = \{I_{i-3}, I_{i-2}, \bar{I}_{i-1}\}$ and the bigger stencil $\Gamma = S_1 \cup S_2 \cup S_3$, we construct $p_n(x)$ $(n = 1, 2, 3)$ and $q(x)$. At the point $x_{i-3+\frac{\sqrt{3}}{6}}$, we have:

$$p_1(x_{i-3+\frac{\sqrt{3}}{6}}) = u_{i-5}^{(0)}\sqrt{3}/12 - u_{i-4}^{(0)}\sqrt{3}/3 + u_{i-3}^{(0)}(4 + \sqrt{3})/4, \tag{C.32}$$

$$p_2(x_{i-3+\frac{\sqrt{3}}{6}}) = -u_{i-4}^{(0)}\sqrt{3}/12 + u_{i-3}^{(0)} + u_{i-2}^{(0)}\sqrt{3}/12, \tag{C.33}$$

$$p_3(x_{i-3+\frac{\sqrt{3}}{6}}) = \left(u_{i-3}^{(0)}(5 + 2\xi)(21 - 5\sqrt{3} + (6 - \sqrt{3})\xi)\right.$$
$$\left. + \sqrt{3}(-6\bar{u}_{i-1}^{(0)} + u_{i-2}^{(0)}(31 + 15\xi + 2\xi^2)))\right)/\left(3(35 + 24\xi + 4\xi^2)\right). \tag{C.34}$$

At the point $x_{i-3-\frac{\sqrt{3}}{6}}$, we have:

$$p_1(x_{i-3-\frac{\sqrt{3}}{6}}) = -u_{i-5}^{(0)}\sqrt{3}/12 + u_{i-4}^{(0)}\sqrt{3}/3 + u_{i-3}^{(0)}(4 - \sqrt{3})/4, \tag{C.35}$$

$$p_2(x_{i-3-\frac{\sqrt{3}}{6}}) = u_{i-4}^{(0)}\sqrt{3}/12 + u_{i-3}^{(0)} - u_{i-2}^{(0)}\sqrt{3}/12, \tag{C.36}$$

$$p_3(x_{i-3-\frac{\sqrt{3}}{6}}) = \left(u_{i-3}^{(0)}(5 + 2\xi)(21 + 5\sqrt{3} + (6 + \sqrt{3})\xi)\right.$$
$$\left. + \sqrt{3}(6\bar{u}_{i-1}^{(0)} - u_{i-2}^{(0)}(31 + 15\xi + 2\xi^2)))\right)/\left(3(35 + 24\xi + 4\xi^2)\right). \tag{C.37}$$

Step C.1.2. We find the combination coefficients. For $x_G = x_{i-3+\frac{\sqrt{3}}{6}}$, the associated linear weights are:

$$\gamma_1 = (84 - \sqrt{3}/3 + 28\xi)/(396 + 72\xi),$$
$$\gamma_2 = \left(6744 + \sqrt{3} + 2(1530 + \sqrt{3})\xi + 264\xi^2\right)/\left(108(99 + 40\xi + 4\xi^2)\right),$$
$$\gamma_3 = (420 + 2\sqrt{3})/\left(27(99 + 40\xi + 4\xi^2)\right). \tag{C.38}$$

For $x_G = x_{i-3-\frac{\sqrt{3}}{6}}$, the associated linear weights are:

$$\gamma_1 = (84 + \sqrt{3}/3 + 28\xi)/(396 + 72\xi),$$
$$\gamma_2 = \left(6744 - \sqrt{3} + 2(1530 - \sqrt{3})\xi + 264\xi^2\right)/\left(108(99 + 40\xi + 4\xi^2)\right),$$
$$\gamma_3 = (420 - 2\sqrt{3})/\left(27(99 + 40\xi + 4\xi^2)\right). \tag{C.39}$$

Step C.2.1. Here, I_{i-2} is the "troubled cell". Given the small stencils $S_1 = \{I_{i-4}, I_{i-3}, I_{i-2}\}$, $S_2 = \{I_{i-3}, I_{i-2}, \bar{I}_{i-1}\}$, $S_3 = \{I_{i-2}, \bar{I}_{i-1}, \bar{I}_{i+1}\}$ and the bigger stencil $\Gamma = S_1 \cup S_2 \cup S_3$, we construct $p_n(x)$ ($n = 1, 2, 3$) and $q(x)$. At the point $x_{i-2+\frac{\sqrt{3}}{6}}$, we have:

$$p_1(x_{i-2+\frac{\sqrt{3}}{6}}) = u_{i-4}^{(0)}\sqrt{3}/12 - u_{i-3}^{(0)}\sqrt{3}/3 + u_{i-2}^{(0)}(4+\sqrt{3})/4, \tag{C.40}$$

$$p_2(x_{i-2+\frac{\sqrt{3}}{6}}) = \big(6\sqrt{3}\bar{u}_{i-1}^{(0)} - \sqrt{3}u_{i-3}^{(0)}\big(10+9\xi+2\xi^2\big) + u_{i-2}^{(0)}\big(105+4\sqrt{3}+9(8+\sqrt{3})\xi$$
$$+ 2(6+\sqrt{3})\xi^2\big)\big)\big/\big(3\big(35+24\xi+4\xi^2\big)\big), \tag{C.41}$$

$$p_3(x_{i-2+\frac{\sqrt{3}}{6}}) = \big(6u_{i-2}^{(0)}\big(6(5-\sqrt{3})+(12-\sqrt{3})\xi\big) - \sqrt{3}\big(\bar{u}_{i+1}^{(0)}\big(10+9\xi+2\xi^2\big)$$
$$- \bar{u}_{i-1}^{(0)}\big(46+15\xi+2\xi^2\big)\big)\big)\big/\big(36(5+2\xi)\big). \tag{C.42}$$

At the point $x_{i-2-\frac{\sqrt{3}}{6}}$, we have:

$$p_1(x_{i-2-\frac{\sqrt{3}}{6}}) = -u_{i-4}^{(0)}\sqrt{3}/12 + u_{i-3}^{(0)}\sqrt{3}/3 + u_{i-2}^{(0)}(4-\sqrt{3})/4, \tag{C.43}$$

$$p_2(x_{i-2-\frac{\sqrt{3}}{6}}) = \big(-6\sqrt{3}\bar{u}_{i-1}^{(0)} + \sqrt{3}u_{i-3}^{(0)}\big(10+9\xi+2\xi^2\big) + u_{i-2}^{(0)}\big(105-4\sqrt{3}+9(8-\sqrt{3})\xi$$
$$+ 2(6-\sqrt{3})\xi^2\big)\big)\big/\big(3\big(35+24\xi+4\xi^2\big)\big), \tag{C.44}$$

$$p_3(x_{i-2-\frac{\sqrt{3}}{6}}) = \big(6u_{i-2}^{(0)}\big(6(5+\sqrt{3})+(12+\sqrt{3})\xi\big) + \sqrt{3}\big(\bar{u}_{i+1}^{(0)}\big(10+9\xi+2\xi^2\big)$$
$$- \bar{u}_{i-1}^{(0)}\big(46+15\xi+2\xi^2\big)\big)\big)\big/\big(36(5+2\xi)\big). \tag{C.45}$$

Step C.2.2. We find the combination coefficients. For $x_G = x_{i-2+\frac{\sqrt{3}}{6}}$, the associated linear weights are:

$$\gamma_1 = (130 - \sqrt{3}/3 + 64\xi)/\big(54(9+2\xi)\big),$$
$$\gamma_2 = \big(35268 + 13\sqrt{3} + 14(1530+\sqrt{3})\xi + 1848\xi^2\big)\big/\big(3240\big(18+13\xi+2\xi^2\big)\big),$$
$$\gamma_3 = (92 + \sqrt{3}/3 + 44\xi)/\big(360(2+\xi)\big). \tag{C.46}$$

For $x_G = x_{i-2-\frac{\sqrt{3}}{6}}$, the associated linear weights are:

$$\gamma_1 = (130 + \sqrt{3}/3 + 64\xi)/\big(54(9+2\xi)\big),$$
$$\gamma_2 = \big(35268 - 13\sqrt{3} + 14(1530-\sqrt{3})\xi + 1848\xi^2\big)\big/\big(3240\big(18+13\xi+2\xi^2\big)\big),$$
$$\gamma_3 = (92 - \sqrt{3}/3 + 44\xi)/\big(360(2+\xi)\big). \tag{C.47}$$

Step C.3.1. Here, $\bar{I}_{i-1}$ is the "troubled cell". Given the small stencils $S_1 = \{I_{i-3}, I_{i-2}, \bar{I}_{i-1}\}$, $S_2 = \{I_{i-2}, \bar{I}_{i-1}, \bar{I}_{i+1}\}$, $S_3 = \{\bar{I}_{i-1}, \bar{I}_{i+1}, I_{i+2}\}$ and the bigger stencil $\Gamma = S_1 \cup S_2 \cup S_3$, we construct $p_n(x)$ ($n = 1, 2, 3$) and $q(x)$. At the point $\bar{x}_{i-1+\frac{\sqrt{3}}{6}}$, we have:

$$p_1(\bar{x}_{i-1+\frac{\sqrt{3}}{6}}) = \big(12\bar{u}_{i-1}^{(0)}(10+3\sqrt{3}+4\xi+2\sqrt{3}\xi) + \sqrt{3}u_{i-3}^{(0)}\big(15+16\xi+4\xi^2\big)$$
$$- \sqrt{3}u_{i-2}^{(0)}\big(51+40\xi+4\xi^2\big)\big)\big/\big(24(5+2\xi)\big), \tag{C.48}$$

$$p_2(\bar{x}_{i-1+\frac{\sqrt{3}}{6}}) = \big(-6\sqrt{3}u_{i-2}^{(0)}\big(27+12\xi-4\xi^2\big) + \sqrt{3}\bar{u}_{i+1}^{(0)}\big(105+142\xi+60\xi^2+8\xi^3\big)$$
$$+ \bar{u}_{i-1}^{(0)}\big(1440+57\sqrt{3}+576\xi-70\sqrt{3}\xi-84\sqrt{3}\xi^2-8\sqrt{3}\xi^3\big)\big)\big/\big(288(5+2\xi)\big), \tag{C.49}$$

$$p_3(\bar{x}_{i-1+\frac{\sqrt{3}}{6}}) = \big(\bar{u}_{i-1}^{(0)}(-5+2\xi)\big(288-75\sqrt{3}-44\sqrt{3}\xi+4\sqrt{3}\xi^2\big)$$
$$- \sqrt{3}(3+2\xi)\big(6u_{i+2}^{(0)}(-9+2\xi)+\bar{u}_{i+1}^{(0)}\big(179-72\xi+4\xi^2\big)\big)\big)\big/\big(288(-5+2\xi)\big). \tag{C.50}$$

At the point $\bar{x}_{i-1-\frac{\sqrt{3}}{6}}$, we have:

$$p_1(\bar{x}_{i-1-\frac{\sqrt{3}}{6}}) = \big(12\bar{u}_{i-1}^{(0)}(10 - 3\sqrt{3} + 4\xi - 2\sqrt{3}\xi) - \sqrt{3}u_{i-3}^{(0)}(15 + 16\xi + 4\xi^2)$$
$$+ \sqrt{3}u_{i-2}^{(0)}(51 + 40\xi + 4\xi^2)\big)/\big(24(5 + 2\xi)\big), \tag{C.51}$$

$$p_2(\bar{x}_{i-1-\frac{\sqrt{3}}{6}}) = \big(6\sqrt{3}u_{i-2}^{(0)}(27 + 12\xi - 4\xi^2) - \sqrt{3}\bar{u}_{i+1}^{(0)}(105 + 142\xi + 60\xi^2 + 8\xi^3)$$
$$+ \bar{u}_{i-1}^{(0)}(1440 - 57\sqrt{3} + 576\xi + 70\sqrt{3}\xi + 84\sqrt{3}\xi^2 + 8\sqrt{3}\xi^3)\big)/\big(288(5 + 2\xi)\big), \tag{C.52}$$

$$p_3(\bar{x}_{i-1-\frac{\sqrt{3}}{6}}) = \big((\bar{u}_{i-1}^{(0)}(-5 + 2\xi)(288 + 75\sqrt{3} + 44\sqrt{3}\xi - 4\sqrt{3}\xi^2))$$
$$+ \sqrt{3}(3 + 2\xi)(6u_{i+2}^{(0)}(-9 + 2\xi) + \bar{u}_{i+1}^{(0)}(179 - 72\xi + 4\xi^2))\big)/\big(288(-5 + 2\xi)\big). \tag{C.53}$$

Step C.3.2. We find the combination coefficients. For $x_G = \bar{x}_{i-1+\frac{\sqrt{3}}{6}}$, the associated linear weights are:

$$\gamma_1 = \big(27 - 1296\sqrt{3} + 6(9 + 8\sqrt{3})\xi + (36 + 96\sqrt{3})\xi^2 + 8\xi^3\big)/\big(720\sqrt{3}(7 + 2\xi)\big),$$
$$\gamma_2 = \big(-27(1452 + \sqrt{3}) - 2088\xi + 72(58 + \sqrt{3})\xi^2$$
$$+ 32(9 + 2\sqrt{3})\xi^3 + 16\sqrt{3}\xi^4\big)/\big(1080(-63 - 4\xi + 4\xi^2)\big),$$
$$\gamma_3 = \big(27 + 1080\sqrt{3} + 6(9 + 56\sqrt{3})\xi + 36\xi^2 + 8\xi^3\big)/\big(720\sqrt{3}(-9 + 2\xi)\big). \tag{C.54}$$

For $x_G = \bar{x}_{i-1-\frac{\sqrt{3}}{6}}$, the associated linear weights are:

$$\gamma_1 = \big(27 + 1296\sqrt{3} + 6(9 - 8\sqrt{3})\xi + (36 - 96\sqrt{3})\xi^2 + 8\xi^3\big)/\big(720\sqrt{3}(7 + 2\xi)\big),$$
$$\gamma_2 = \big(-27(1452 - \sqrt{3}) - 2088\xi + 72(58 - \sqrt{3})\xi^2 + 32(9 - 2\sqrt{3})\xi^3 - 16\sqrt{3}\xi^4\big)$$
$$/\big(1080(-63 - 4\xi + 4\xi^2)\big),$$
$$\gamma_3 = \big(27 - 1080\sqrt{3} + 6(9 - 56\sqrt{3})\xi + 36\xi^2 + 8\xi^3\big)/\big(720\sqrt{3}(-9 + 2\xi)\big). \tag{C.55}$$

Step C.4.1. Here, $\bar{I}_{i+1}$ is the "troubled cell". Given the small stencils $S_1 = \{I_{i-2}, \bar{I}_{i-1}, \bar{I}_{i+1}\}$, $S_2 = \{\bar{I}_{i-1}, \bar{I}_{i+1}, I_{i+2}\}$, $S_3 = \{\bar{I}_{i+1}, I_{i+2}, I_{i+3}\}$ and the bigger stencil $\Gamma = S_1 \cup S_2 \cup S_3$, we construct $p_n(x)$ ($n = 1, 2, 3$) and $q(x)$. At the point $\bar{x}_{i+1+\frac{\sqrt{3}}{6}}$, we have:

$$p_1(\bar{x}_{i+1+\frac{\sqrt{3}}{6}}) = \big(-6\sqrt{3}u_{i-2}^{(0)}(-27 + 12\xi + 4\xi^2) + \bar{u}_{i+1}^{(0)}(5 + 2\xi)(288 + 75\sqrt{3} - 44\sqrt{3}\xi$$
$$- 4\sqrt{3}\xi^2) + \sqrt{3}\bar{u}_{i-1}^{(0)}(-537 + 142\xi + 132\xi^2 + 8\xi^3)\big)/\big(288(5 + 2\xi)\big), \tag{C.56}$$

$$p_2(\bar{x}_{i+1+\frac{\sqrt{3}}{6}}) = \big(6\sqrt{3}u_{i+2}^{(0)}(-27 + 12\xi + 4\xi^2) + \sqrt{3}\bar{u}_{i-1}^{(0)}(105 - 142\xi + 60\xi^2 - 8\xi^3)$$
$$+ \bar{u}_{i+1}^{(0)}(-1440 + 57\sqrt{3} + 576\xi + 70\sqrt{3}\xi - 84\sqrt{3}\xi^2 + 8\sqrt{3}\xi^3)\big)/\big(288(-5 + 2\xi)\big), \tag{C.57}$$

$$p_3(\bar{x}_{i+1+\frac{\sqrt{3}}{6}}) = \big(12\bar{u}_{i+1}^{(0)}(-10 + 3\sqrt{3} + 2(2 - \sqrt{3})\xi) + \sqrt{3}(-3 + 2\xi)(u_{i+2}^{(0)}(17 - 2\xi)$$
$$- u_{i+3}^{(0)}(5 - 2\xi))\big)/\big(24(-5 + 2\xi)\big). \tag{C.58}$$

At the point $\bar{x}_{i+1-\frac{\sqrt{3}}{6}}$, we have:

$$p_1(\bar{x}_{i+1-\frac{\sqrt{3}}{6}}) = \big(6\sqrt{3}u_{i-2}^{(0)}(-27 + 12\xi + 4\xi^2) + \bar{u}_{i+1}^{(0)}(5 + 2\xi)(288 - 75\sqrt{3} + 44\sqrt{3}\xi + 4\sqrt{3}\xi^2)$$
$$- \sqrt{3}\bar{u}_{i-1}^{(0)}(-537 + 142\xi + 132\xi^2 + 8\xi^3)\big)/\big(288(5 + 2\xi)\big), \tag{C.59}$$

$$p_2(\bar{x}_{i+1-\frac{\sqrt{3}}{6}}) = \big(-6\sqrt{3}u_{i+2}^{(0)}(-27 + 12\xi + 4\xi^2) - \sqrt{3}\bar{u}_{i-1}^{(0)}(105 - 142\xi + 60\xi^2 - 8\xi^3)$$
$$+ \bar{u}_{i+1}^{(0)}(-1440 - 57\sqrt{3} + 576\xi - 70\sqrt{3}\xi + 84\sqrt{3}\xi^2 - 8\sqrt{3}\xi^3)\big)/\big(288(-5 + 2\xi)\big), \tag{C.60}$$

$$p_3(\bar{x}_{i+1-\frac{\sqrt{3}}{6}}) = \big(12\bar{u}_{i+1}^{(0)}(-10 - 3\sqrt{3} + 2(2 + \sqrt{3})\xi) - \sqrt{3}(-3 + 2\xi)(u_{i+2}^{(0)}(17 - 2\xi)$$
$$- u_{i+3}^{(0)}(5 - 2\xi))\big)/\big(24(-5 + 2\xi)\big). \tag{C.61}$$

Step C.4.2. We find the combination coefficients. For $x_G = \bar{x}_{i+1+\frac{\sqrt{3}}{6}}$, the associated linear weights are:

$$\gamma_1 = \left(-27 + 1080\sqrt{3} + 54\xi - 336\sqrt{3}\xi - 36\xi^2 + 8\xi^3\right)\big/\left(720\sqrt{3}(9 + 2\xi)\right),$$

$$\gamma_2 = \left(-27(1452 - \sqrt{3}) + 2088\xi + 72(58 - \sqrt{3})\xi^2 - 32(9 - 2\sqrt{3})\xi^3 - 16\sqrt{3}\xi^4\right)\big/\left(1080(-63 + 4\xi + 4\xi^2)\right),$$

$$\gamma_3 = \left(-27 - 1296\sqrt{3} - 6(-9 + 8\sqrt{3})\xi + 12(-3 + 8\sqrt{3})\xi^2 + 8\xi^3\right)\big/\left(720\sqrt{3}(-7 + 2\xi)\right). \tag{C.62}$$

For $x_G = \bar{x}_{i+1-\frac{\sqrt{3}}{6}}$, the associated linear weights are:

$$\gamma_1 = \left(27 + 1080\sqrt{3} - 54\xi - 336\sqrt{3}\xi + 36\xi^2 - 8\xi^3\right)\big/\left(720\sqrt{3}(9 + 2\xi)\right),$$

$$\gamma_2 = \left(-27(1452 + \sqrt{3}) + 2088\xi + 72(58 + \sqrt{3})\xi^2 - 32(9 + 2\sqrt{3})\xi^3 + 16\sqrt{3}\xi^4\right)\big/\left(1080(-63 + 4\xi + 4\xi^2)\right),$$

$$\gamma_3 = \left(27 - 1296\sqrt{3} - 6(9 + 8\sqrt{3})\xi + 12(3 + 8\sqrt{3})\xi^2 - 8\xi^3\right)\big/\left(720\sqrt{3}(-7 + 2\xi)\right). \tag{C.63}$$

Step C.5.1. Here, I_{i+2} is the "troubled cell". Given the small stencils $S_1 = \{\bar{I}_{i-1}, \bar{I}_{i+1}, I_{i+2}\}$, $S_2 = \{\bar{I}_{i+1}, I_{i+2}, I_{i+3}\}$, $S_3 = \{I_{i+2}, I_{i+3}, I_{i+4}\}$ and the bigger stencil $\Gamma = S_1 \cup S_2 \cup S_3$, we construct $p_n(x)$ ($n = 1, 2, 3$) and $q(x)$. At the point $x_{i+2+\frac{\sqrt{3}}{6}}$, we have:

$$p_1(x_{i+2+\frac{\sqrt{3}}{6}}) = \left(6u_{i+2}^{(0)}(-30 - 6\sqrt{3} + 12\xi + \sqrt{3}\xi) - \sqrt{3}\bar{u}_{i-1}^{(0)}(10 - 9\xi + 2\xi^2)\right.$$
$$\left. + \sqrt{3}\bar{u}_{i+1}^{(0)}(46 - 15\xi + 2\xi^2)\right)\big/\left(36(-5 + 2\xi)\right), \tag{C.64}$$

$$p_2(x_{i+2+\frac{\sqrt{3}}{6}}) = \left(-6\sqrt{3}\bar{u}_{i+1}^{(0)} + \sqrt{3}u_{i+3}^{(0)}(10 - 9\xi + 2\xi^2) + u_{i+2}^{(0)}(105 - 4\sqrt{3} - 9(8 - \sqrt{3})\xi\right.$$
$$\left. + 2(6 - \sqrt{3})\xi^2)\right)\big/\left(3(35 - 24\xi + 4\xi^2)\right), \tag{C.65}$$

$$p_3(x_{i+2+\frac{\sqrt{3}}{6}}) = u_{i+2}^{(0)}(4 - \sqrt{3})/4 + \left(4u_{i+3}^{(0)} - u_{i+4}^{(0)}\right)\sqrt{3}/12. \tag{C.66}$$

At the point $x_{i+2-\frac{\sqrt{3}}{6}}$, we have:

$$p_1(x_{i+2-\frac{\sqrt{3}}{6}}) = \left(6u_{i+2}^{(0)}(-30 + 6\sqrt{3} + 12\xi - \sqrt{3}\xi) + \sqrt{3}\bar{u}_{i-1}^{(0)}(10 - 9\xi + 2\xi^2)\right.$$
$$\left. - \sqrt{3}\bar{u}_{i+1}^{(0)}(46 - 15\xi + 2\xi^2)\right)\big/\left(36(-5 + 2\xi)\right), \tag{C.67}$$

$$p_2(x_{i+2-\frac{\sqrt{3}}{6}}) = \left(6\sqrt{3}\bar{u}_{i+1}^{(0)} - \sqrt{3}u_{i+3}^{(0)}(10 - 9\xi + 2\xi^2) + u_{i+2}^{(0)}(105 + 4\sqrt{3} - 9(8 + \sqrt{3})\xi\right.$$
$$\left. + 2(6 + \sqrt{3})\xi^2)\right)\big/\left(3(35 - 24\xi + 4\xi^2)\right), \tag{C.68}$$

$$p_3(x_{i+2-\frac{\sqrt{3}}{6}}) = u_{i+2}^{(0)}(4 + \sqrt{3})/4 - \left(4u_{i+3}^{(0)} - u_{i+4}^{(0)}\right)\sqrt{3}/12. \tag{C.69}$$

Step C.5.2. We find the combination coefficients. For $x_G = x_{i+2+\frac{\sqrt{3}}{6}}$, the associated linear weights are:

$$\gamma_1 = (-276 + \sqrt{3} + 132\xi)\big/\left(1080(-2 + \xi)\right),$$

$$\gamma_2 = \left(35268 - 13\sqrt{3} - 14(1530 - \sqrt{3})\xi + 1848\xi^2\right)\big/\left(3240(18 - 13\xi + 2\xi^2)\right),$$

$$\gamma_3 = (390 + \sqrt{3} - 192\xi)\big/\left(162(9 - 2\xi)\right). \tag{C.70}$$

For $x_G = x_{i+2-\frac{\sqrt{3}}{6}}$, the associated linear weights are:

$$\gamma_1 = (-276 - \sqrt{3} + 132\xi)\big/\left(1080(-2 + \xi)\right),$$

$$\gamma_2 = \left(35268 + 13\sqrt{3} - 14(1530 + \sqrt{3})\xi + 1848\xi^2\right)\big/\left(3240(18 - 13\xi + 2\xi^2)\right),$$

$$\gamma_3 = (390 - \sqrt{3} - 192\xi)\big/\left(162(9 - 2\xi)\right). \tag{C.71}$$

Step C.6.1. Here, I_{i+3} is the "troubled cell". Given the small stencils $S_1 = \{\bar{I}_{i+1}, I_{i+2}, I_{i+3}\}$, $S_2 = \{I_{i+2}, I_{i+3}, I_{i+4}\}$, $S_3 = \{I_{i+3}, I_{i+4}, I_{i+5}\}$ and the bigger stencil $\Gamma = S_1 \cup S_2 \cup S_3$, we construct $p_n(x)$ ($n = 1, 2, 3$) and $q(x)$. At the point $x_{i+3+\frac{\sqrt{3}}{6}}$, we have:

$$p_1(x_{i+3+\frac{\sqrt{3}}{6}}) = \left(6\sqrt{3}\bar{u}_{i+1}^{(0)} - u_{i+3}^{(0)}(-5+2\xi)(21+5\sqrt{3}-(6+\sqrt{3})\xi)\right.$$
$$\left. - \sqrt{3}u_{i+2}^{(0)}(31-15\xi+2\xi^2)\right)/(3(35-24\xi+4\xi^2)), \tag{C.72}$$

$$p_2(x_{i+3+\frac{\sqrt{3}}{6}}) = -u_{i+2}^{(0)}\sqrt{3}/12 + u_{i+3}^{(0)} + u_{i+4}^{(0)}\sqrt{3}/12, \tag{C.73}$$

$$p_3(x_{i+3+\frac{\sqrt{3}}{6}}) = u_{i+3}^{(0)}(4-\sqrt{3})/4 + (4u_{i+4}^{(0)} - u_{i+5}^{(0)})\sqrt{3}/12. \tag{C.74}$$

At the point $x_{i+3-\frac{\sqrt{3}}{6}}$, we have:

$$p_1(x_{i+3-\frac{\sqrt{3}}{6}}) = \left(-6\sqrt{3}\bar{u}_{i+1}^{(0)} - u_{i+3}^{(0)}(-5+2\xi)(21-5\sqrt{3}-(6-\sqrt{3})\xi)\right.$$
$$\left. + \sqrt{3}u_{i+2}^{(0)}(31-15\xi+2\xi^2)\right)/(3(35-24\xi+4\xi^2)), \tag{C.75}$$

$$p_2(x_{i+3-\frac{\sqrt{3}}{6}}) = u_{i+2}^{(0)}\sqrt{3}/12 + u_{i+3}^{(0)} - u_{i+4}^{(0)}\sqrt{3}/12, \tag{C.76}$$

$$p_3(x_{i+3-\frac{\sqrt{3}}{6}}) = u_{i+3}^{(0)}(4+\sqrt{3})/4 - (4u_{i+4}^{(0)} - u_{i+5}^{(0)})\sqrt{3}/12. \tag{C.77}$$

Step C.6.2. We find the combination coefficients. For $x_G = x_{i+3+\frac{\sqrt{3}}{6}}$, the associated linear weights are:

$$\gamma_1 = (420 - 2\sqrt{3})/(27(99-40\xi+4\xi^2)),$$
$$\gamma_2 = (6744 - \sqrt{3} - 2(1530-\sqrt{3})\xi + 264\xi^2)/(108(99-40\xi+4\xi^2)),$$
$$\gamma_3 = (252 + \sqrt{3} - 84\xi)/(1188-216\xi). \tag{C.78}$$

For $x_G = x_{i+3-\frac{\sqrt{3}}{6}}$, the associated linear weights are:

$$\gamma_1 = (420 + 2\sqrt{3})/(27(99-40\xi+4\xi^2)),$$
$$\gamma_2 = (6744 + \sqrt{3} - 2(1530+\sqrt{3})\xi + 264\xi^2)/(108(99-40\xi+4\xi^2)),$$
$$\gamma_3 = (252 - \sqrt{3} - 84\xi)/(1188-216\xi). \tag{C.79}$$

Appendix D. HWENO5 as limiter for application of RKDG3 (HWENO5-RKDG3) to interfacial cell

Step D.1.1. Here, I_{i-2} is the "troubled cell". Given the small stencils $S_1 = \{I_{i-3}, I_{i-2}\}$, $S_2 = \{I_{i-2}, \bar{I}_{i-1}\}$, $S_3 = \{I_{i-3}, I_{i-2}, \bar{I}_{i-1}\}$ and the bigger stencil $\Gamma = S_1 \cup S_2 \cup S_3$, we construct $p_n(x)$ ($n = 1, 2, 3$) and $q(x)$. At the point $x_{i-2+\frac{\sqrt{3}}{6}}$, we have:

$$p_1(x_{i-2+\frac{\sqrt{3}}{6}}) = -u_{i-3}^{(0)}\sqrt{3}/3 + u_{i-2}^{(0)}(3+\sqrt{3})/3 - u_{i-3}^{(1)}\sqrt{3}/6, \tag{D.80}$$

$$p_2(x_{i-2+\frac{\sqrt{3}}{6}}) = \left(3u_{i-2}^{(0)}(3+2\xi)(7-2\sqrt{3}+2\xi) + 4\sqrt{3}(3\bar{u}_{i-1}^{(0)} - \bar{u}_{i-1}^{(1)}(2+\xi))\right)$$
$$/(63+60\xi+12\xi^2), \tag{D.81}$$

$$p_3(x_{i-2+\frac{\sqrt{3}}{6}}) = \left(6\sqrt{3}\bar{u}_{i-1}^{(0)} - \sqrt{3}u_{i-3}^{(0)}(10+9\xi+2\xi^2) + u_{i-2}^{(0)}(105+4\sqrt{3}+9(8+\sqrt{3})\xi\right.$$
$$\left. + 2(6+\sqrt{3})\xi^2)\right)/(3(35+24\xi+4\xi^2)). \tag{D.82}$$

At the point $x_{i-2-\frac{\sqrt{3}}{6}}$, we have:

$$p_1(x_{i-2-\frac{\sqrt{3}}{6}}) = u_{i-3}^{(0)}\sqrt{3}/3 + u_{i-2}^{(0)}(3-\sqrt{3})/3 + u_{i-3}^{(1)}\sqrt{3}/6, \tag{D.83}$$

$$p_2(x_{i-2-\frac{\sqrt{3}}{6}}) = \left(3u_{i-2}^{(0)}(3+2\xi)(7+2\sqrt{3}+2\xi) - 4\sqrt{3}(3\bar{u}_{i-1}^{(0)} - \bar{u}_{i-1}^{(1)}(2+\xi))\right)$$
$$/(63+60\xi+12\xi^2), \tag{D.84}$$

$$p_3(x_{i-2-\frac{\sqrt{3}}{6}}) = \left(-6\sqrt{3}\bar{u}_{i-1}^{(0)} + \sqrt{3}u_{i-3}^{(0)}(10+9\xi+2\xi^2) + u_{i-2}^{(0)}(105-4\sqrt{3}+9(8-\sqrt{3})\xi\right.$$
$$\left. + 2(6-\sqrt{3})\xi^2)\right)/(3(35+24\xi+4\xi^2)). \tag{D.85}$$

Step D.1.2. We find the combination coefficients. For $x_G = x_{i-2+\frac{\sqrt{3}}{6}}$, the associated linear weights are:

$$\gamma_1 = \big(29877 - 197\sqrt{3} + (42876 - 96\sqrt{3})\xi + 12(1872 - \sqrt{3})\xi^2 + 5136\xi^3 + 432\xi^4\big)$$
$$\big/\big(9(8613 + 9204\xi + 3744\xi^2 + 688\xi^3 + 48\xi^4)\big),$$
$$\gamma_2 = \big((7 + 2\xi)(91 + 3488\sqrt{3} + 30(1 + 92\sqrt{3})\xi + 528\sqrt{3}\xi^2)\big)$$
$$\big/\big(6\sqrt{3}(2 + \xi)(8613 + 9204\xi + 3744\xi^2 + 688\xi^3 + 48\xi^4)\big),$$
$$\gamma_3 = \big(117312 + 151\sqrt{3} + (176232 + 386\sqrt{3})\xi + 180(540 + \sqrt{3})\xi^2 + 24(980 + \sqrt{3})\xi^3 + 2112\xi^4\big)$$
$$\big/\big(18(17226 + 27021\xi + 16692\xi^2 + 5120\xi^3 + 784\xi^4 + 48\xi^5)\big). \tag{D.86}$$

For $x_G = x_{i-2-\frac{\sqrt{3}}{6}}$, the associated linear weights are:

$$\gamma_1 = \big(29877 + 197\sqrt{3} + (42876 + 96\sqrt{3})\xi + 12(1872 + \sqrt{3})\xi^2 + 5136\xi^3 + 432\xi^4\big)$$
$$\big/\big(9(8613 + 9204\xi + 3744\xi^2 + 688\xi^3 + 48\xi^4)\big),$$
$$\gamma_2 = \big((7 + 2\xi)(-91 + 3488\sqrt{3} + 30(-1 + 92\sqrt{3})\xi + 528\sqrt{3}\xi^2)\big)$$
$$\big/\big(6\sqrt{3}(2 + \xi)(8613 + 9204\xi + 3744\xi^2 + 688\xi^3 + 48\xi^4)\big),$$
$$\gamma_3 = \big(117312 - 151\sqrt{3} + (176232 - 386\sqrt{3})\xi + 180(540 - \sqrt{3})\xi^2 + 24(980 - \sqrt{3})\xi^3 + 2112\xi^4\big)$$
$$\big/\big(18(17226 + 27021\xi + 16692\xi^2 + 5120\xi^3 + 784\xi^4 + 48\xi^5)\big). \tag{D.87}$$

Step D.2.1. Here, $\bar{I}_{i-1}$ is the "troubled cell". Given the small stencils $S_1 = \{I_{i-2}, \bar{I}_{i-1}\}$, $S_2 = \{\bar{I}_{i-1}, \bar{I}_{i+1}\}$, $S_3 = \{I_{i-2}, \bar{I}_{i-1}, \bar{I}_{i+1}\}$ and the bigger stencil $\Gamma = S_1 \cup S_2 \cup S_3$, we construct $p_n(x)$ $(n = 1, 2, 3)$ and $q(x)$. At the point $\bar{x}_{i-1+\frac{\sqrt{3}}{6}}$, we have:

$$p_1(\bar{x}_{i-1+\frac{\sqrt{3}}{6}}) = \big(-12\sqrt{3}u_{i-2}^{(0)}(3 + 2\xi) + 12\bar{u}_{i-1}^{(0)}(8 + 3\sqrt{3} + 2(2 + \sqrt{3})\xi)$$
$$- \sqrt{3}u_{i-2}^{(1)}(21 + 20\xi + 4\xi^2)\big)\big/(48(2 + \xi)), \tag{D.88}$$
$$p_2(\bar{x}_{i-1+\frac{\sqrt{3}}{6}}) = \big(12\bar{u}_{i-1}^{(0)}(-3 + 2\xi)(3(3 - \sqrt{3}) + 2(1 - \sqrt{3})\xi)$$
$$- \sqrt{3}(3 + 2\xi)^2(\bar{u}_{i+1}^{(1)}(-9 + 2\xi) + 6\bar{u}_{i+1}^{(0)}(3 + 2\xi))\big)\big/(6(-81 - 18\xi + 36\xi^2 + 8\xi^3)), \tag{D.89}$$
$$p_3(\bar{x}_{i-1+\frac{\sqrt{3}}{6}}) = \big(-6\sqrt{3}u_{i-2}^{(0)}(27 + 12\xi - 4\xi^2) + \sqrt{3}\bar{u}_{i+1}^{(0)}(105 + 142\xi + 60\xi^2 + 8\xi^3)$$
$$+ \bar{u}_{i-1}^{(0)}(1440 + 57\sqrt{3} + 576\xi - 70\sqrt{3}\xi - 84\sqrt{3}\xi^2 - 8\sqrt{3}\xi^3)\big)\big/(288(5 + 2\xi)). \tag{D.90}$$

At the point $\bar{x}_{i-1-\frac{\sqrt{3}}{6}}$, we have:

$$p_1(\bar{x}_{i-1-\frac{\sqrt{3}}{6}}) = \big(12\sqrt{3}u_{i-2}^{(0)}(3 + 2\xi) + 12\bar{u}_{i-1}^{(0)}(8 - 3\sqrt{3} + 2(2 - \sqrt{3})\xi) + \sqrt{3}u_{i-2}^{(1)}(21 + 20\xi + 4\xi^2)\big)$$
$$\big/(48(2 + \xi)), \tag{D.91}$$
$$p_2(\bar{x}_{i-1-\frac{\sqrt{3}}{6}}) = \big(12\bar{u}_{i-1}^{(0)}(-3 + 2\xi)(3(3 + \sqrt{3}) + 2(1 + \sqrt{3})\xi)$$
$$+ \sqrt{3}(3 + 2\xi)^2(\bar{u}_{i+1}^{(1)}(-9 + 2\xi) + 6\bar{u}_{i+1}^{(0)}(3 + 2\xi))\big)\big/(6(-81 - 18\xi + 36\xi^2 + 8\xi^3)), \tag{D.92}$$
$$p_3(\bar{x}_{i-1-\frac{\sqrt{3}}{6}}) = \big(6\sqrt{3}u_{i-2}^{(0)}(27 + 12\xi - 4\xi^2) - \sqrt{3}\bar{u}_{i+1}^{(0)}(105 + 142\xi + 60\xi^2 + 8\xi^3)$$
$$+ \bar{u}_{i-1}^{(0)}(1440 - 57\sqrt{3} + 576\xi + 70\sqrt{3}\xi + 84\sqrt{3}\xi^2 + 8\sqrt{3}\xi^3)\big)\big/(288(5 + 2\xi)). \tag{D.93}$$

Step D.2.2. We find the combination coefficients. For $x_G = \bar{x}_{i-1+\frac{\sqrt{3}}{6}}$, the associated linear weights are:

$$\gamma_1 = -\big((2 + \xi)(-891(-9 + 212\sqrt{3}) + (18846 - 72216\sqrt{3})\xi - 24(-693 + 52\sqrt{3})\xi^2$$
$$+ 16(423 + 292\sqrt{3})\xi^3 + 16(79 + 84\sqrt{3})\xi^4 + 32(3 + 4\sqrt{3})\xi^5)\big)$$
$$\big/\big(6\sqrt{3}(168399 + 211942\xi + 104600\xi^2 + 26928\xi^3 + 3760\xi^4 + 224\xi^5)\big),$$

$$\gamma_2 = -\big((9+2\xi)\big(3807 + 70704\sqrt{3} + 96(99+749\sqrt{3})\xi + (8856+21824\sqrt{3})\xi^2 + 64(57+26\sqrt{3})\xi^3$$
$$+ 560\xi^4\big)\big)\big/\big(12\sqrt{3}(-216513 - 162522\xi - 27496\xi^2 + 3120\xi^3 + 1968\xi^4 + 224\xi^5)\big),$$
$$\gamma_3 = \big(81(-85588 - 201\sqrt{3}) - 18(420388 + 705\sqrt{3})\xi - 12(186668 - 3393\sqrt{3})\xi^2$$
$$+ 8(31052 + 9027\sqrt{3})\xi^3 + (280640 + 46928\sqrt{3})\xi^4 + 96(764 + 151\sqrt{3})\xi^5$$
$$+ 64(148 + 33\sqrt{3})\xi^6 + 128(4+\sqrt{3})\xi^7\big)\big/\big(12(-1515591 - 1570680\xi - 517516\xi^2$$
$$- 33152\xi^3 + 20016\xi^4 + 5504\xi^5 + 448\xi^6)\big). \tag{D.94}$$

For $x_G = \bar{x}_{i-1-\frac{\sqrt{3}}{6}}$, the associated linear weights are:

$$\gamma_1 = -\big((2+\xi)\big(-891(9+212\sqrt{3}) + (-18846 - 72216\sqrt{3})\xi - 24(693 + 52\sqrt{3})\xi^2$$
$$+ 16(-423 + 292\sqrt{3})\xi^3 + 16(-79 + 84\sqrt{3})\xi^4 + 32(-3 + 4\sqrt{3})\xi^5\big)$$
$$\big/\big(6\sqrt{3}(168399 + 211942\xi + 104600\xi^2 + 26928\xi^3 + 3760\xi^4 + 224\xi^5)\big),$$
$$\gamma_2 = \big((9+2\xi)\big(3807 - 70704\sqrt{3} + 96(99 - 749\sqrt{3})\xi + (8856 - 21824\sqrt{3})\xi^2 + 64(57 - 26\sqrt{3})\xi^3$$
$$+ 560\xi^4\big)\big)\big/\big(12\sqrt{3}(-216513 - 162522\xi - 27496\xi^2 + 3120\xi^3 + 1968\xi^4 + 224\xi^5)\big),$$
$$\gamma_3 = \big(81(-85588 + 201\sqrt{3}) - 18(420388 - 705\sqrt{3})\xi - 12(186668 + 3393\sqrt{3})\xi^2 + 8(31052 - 9027\sqrt{3})\xi^3$$
$$+ (280640 - 46928\sqrt{3})\xi^4 + 96(764 - 151\sqrt{3})\xi^5 + 64(148 - 33\sqrt{3})\xi^6 + 128(4 - \sqrt{3})\xi^7\big)$$
$$\big/\big(12(-1515591 - 1570680\xi - 517516\xi^2 - 33152\xi^3 + 20016\xi^4 + 5504\xi^5 + 448\xi^6)\big). \tag{D.95}$$

Step D.3.1. Here, $\bar{I}_{i+1}$ is the "troubled cell". Given the small stencils $S_1 = \{\bar{I}_{i-1}, \bar{I}_{i+1}\}$, $S_2 = \{\bar{I}_{i+1}, I_{i+2}\}$, $S_3 = \{\bar{I}_{i-1}, \bar{I}_{i+1}, I_{i+2}\}$ and the bigger stencil $\Gamma = S_1 \cup S_2 \cup S_3$, we construct $p_n(x)$ ($n = 1, 2, 3$) and $q(x)$. At the point $\bar{x}_{i+1+\frac{\sqrt{3}}{6}}$, we have:

$$p_1(\bar{x}_{i+1+\frac{\sqrt{3}}{6}}) = \big(6\bar{u}^{(0)}_{i+1}(3+2\xi)\big(-9 - 3\sqrt{3} + 2(1+\sqrt{3})\xi\big) + 6\sqrt{3}\bar{u}^{(0)}_{i-1}(9 - 4\xi^2)$$
$$+ \sqrt{3}\bar{u}^{(1)}_{i-1}(27 - 12\xi - 4\xi^2)\big)\big/\big(6(-27 - 12\xi + 4\xi^2)\big), \tag{D.96}$$
$$p_2(\bar{x}_{i+1+\frac{\sqrt{3}}{6}}) = \big(12\bar{u}^{(0)}_{i+1}(3+2\xi)\big(8 - 3\sqrt{3} - 2(2-\sqrt{3})\xi\big) + \sqrt{3}(3 - 2\xi)^2\big(u^{(1)}_{i+2}(-7 + 2\xi)$$
$$+ 6u^{(0)}_{i+2}(3 - 2\xi)\big)\big)\big/\big(48(6 - 7\xi + 2\xi^2)\big), \tag{D.97}$$
$$p_3(\bar{x}_{i+1+\frac{\sqrt{3}}{6}}) = \big(6\sqrt{3}u^{(0)}_{i+2}(-27 + 12\xi + 4\xi^2) + \sqrt{3}\bar{u}^{(0)}_{i-1}(105 - 142\xi + 60\xi^2 - 8\xi^3)$$
$$+ \bar{u}^{(0)}_{i+1}(-1440 + 57\sqrt{3} + 576\xi + 70\sqrt{3}\xi - 84\sqrt{3}\xi^2 + 8\sqrt{3}\xi^3)\big)\big/\big(288(-5 + 2\xi)\big). \tag{D.98}$$

At the point $\bar{x}_{i+1-\frac{\sqrt{3}}{6}}$, we have:

$$p_1(\bar{x}_{i+1-\frac{\sqrt{3}}{6}}) = \big(6\bar{u}^{(0)}_{i+1}(3+2\xi)\big(-9 + 3\sqrt{3} + 2(1-\sqrt{3})\xi\big) - 6\sqrt{3}\bar{u}^{(0)}_{i-1}(9 - 4\xi^2)$$
$$- \sqrt{3}\bar{u}^{(1)}_{i-1}(27 - 12\xi - 4\xi^2)\big)\big/\big(6(-27 - 12\xi + 4\xi^2)\big), \tag{D.99}$$
$$p_2(\bar{x}_{i+1-\frac{\sqrt{3}}{6}}) = \big(12\bar{u}^{(0)}_{i+1}(3+2\xi)\big(8 + 3\sqrt{3} - 2(2+\sqrt{3})\xi\big) - \sqrt{3}(3 - 2\xi)^2\big(u^{(1)}_{i+2}(-7 + 2\xi)$$
$$+ 6u^{(0)}_{i+2}(3 - 2\xi)\big)\big)\big/\big(48(6 - 7\xi + 2\xi^2)\big), \tag{D.100}$$
$$p_3(\bar{x}_{i+1-\frac{\sqrt{3}}{6}}) = \big(-6\sqrt{3}u^{(0)}_{i+2}(-27 + 12\xi + 4\xi^2) - \sqrt{3}\bar{u}^{(0)}_{i-1}(105 - 142\xi + 60\xi^2 - 8\xi^3)$$
$$+ \bar{u}^{(0)}_{i+1}(-1440 - 57\sqrt{3} + 576\xi - 70\sqrt{3}\xi + 84\sqrt{3}\xi^2 - 8\sqrt{3}\xi^3)\big)\big/\big(288(-5 + 2\xi)\big). \tag{D.101}$$

Step D.3.2. We find the combination coefficients. For $x_G = \bar{x}_{i+1+\frac{\sqrt{3}}{6}}$, the associated linear weights are:

$$\gamma_1 = \big((-9+2\xi)\big(3807 - 70704\sqrt{3} + 96(-99 + 749\sqrt{3})\xi + (8856 - 21824\sqrt{3})\xi^2 + 64(-57 + 26\sqrt{3})\xi^3$$
$$+ 560\xi^4\big)\big)\big/\big(12\sqrt{3}(216513 - 162522\xi + 27496\xi^2 + 3120\xi^3 - 1968\xi^4 + 224\xi^5)\big),$$

$$\gamma_2 = \big((-2+\xi)(891(9+212\sqrt{3}) + (-18846 - 72216\sqrt{3})\xi + 24(693 + 52\sqrt{3})\xi^2$$
$$+ 16(-423 + 292\sqrt{3})\xi^3 - 16(-79 + 84\sqrt{3})\xi^4 + 32(-3 + 4\sqrt{3})\xi^5)\big)$$
$$\big/ \big(6\sqrt{3}(-168399 + 211942\xi - 104600\xi^2 + 26928\xi^3 - 3760\xi^4 + 224\xi^5)\big),$$
$$\gamma_3 = \big(-81(85588 - 201\sqrt{3}) + 18(420388 - 705\sqrt{3})\xi - 12(186668 + 3393\sqrt{3})\xi^2 - 8(31052 - 9027\sqrt{3})\xi^3$$
$$+ (280640 - 46928\sqrt{3})\xi^4 - 96(764 - 151\sqrt{3})\xi^5 + 64(148 - 33\sqrt{3})\xi^6 - 128(4 - \sqrt{3})\xi^7\big)$$
$$\big/ \big(12(-1515591 + 1570680\xi - 517516\xi^2 + 33152\xi^3 + 20016\xi^4 - 5504\xi^5 + 448\xi^6)\big). \tag{D.102}$$

For $x_G = \bar{x}_{i+1-\frac{\sqrt{3}}{6}}$, the associated linear weights are:

$$\gamma_1 = \big((-9+2\xi)(-3807 - 70704\sqrt{3} + 96(99 + 749\sqrt{3})\xi + (-8856 - 21824\sqrt{3})\xi^2 + 64(57 + 26\sqrt{3})\xi^3$$
$$- 560\xi^4)\big) \big/ \big(12\sqrt{3}(216513 - 162522\xi + 27496\xi^2 + 3120\xi^3 - 1968\xi^4 + 224\xi^5)\big),$$
$$\gamma_2 = \big((-2+\xi)(891(-9 + 212\sqrt{3}) + (18846 - 72216\sqrt{3})\xi + 24(-693 + 52\sqrt{3})\xi^2$$
$$+ 16(423 + 292\sqrt{3})\xi^3 - 16(79 + 84\sqrt{3})\xi^4 + 32(3 + 4\sqrt{3})\xi^5)\big)$$
$$\big/ \big(6\sqrt{3}(-168399 + 211942\xi - 104600\xi^2 + 26928\xi^3 - 3760\xi^4 + 224\xi^5)\big),$$
$$\gamma_3 = \big(-81(85588 + 201\sqrt{3}) + 18(420388 + 705\sqrt{3})\xi - 12(186668 - 3393\sqrt{3})\xi^2 - 8(31052 + 9027\sqrt{3})\xi^3$$
$$+ (280640 + 46928\sqrt{3})\xi^4 - 96(764 + 151\sqrt{3})\xi^5 + 64(148 + 33\sqrt{3})\xi^6 - 128(4 + \sqrt{3})\xi^7\big)$$
$$\big/ \big(12(-1515591 + 1570680\xi - 517516\xi^2 + 33152\xi^3 + 20016\xi^4 - 5504\xi^5 + 448\xi^6)\big). \tag{D.103}$$

Step D.4.1. Here, I_{i+2} is the "troubled cell". Given the small stencils $S_1 = \{\bar{I}_{i+1}, I_{i+2}\}$, $S_2 = \{I_{i+2}, I_{i+3}\}$, $S_3 = \{\bar{I}_{i+1}, I_{i+2}, I_{i+3}\}$ and the bigger stencil $\Gamma = S_1 \cup S_2 \cup S_3$, we construct $p_n(x)$ ($n = 1, 2, 3$) and $q(x)$. At the point $x_{i+2+\frac{\sqrt{3}}{6}}$, we have:

$$p_1(x_{i+2+\frac{\sqrt{3}}{6}}) = \big(4\sqrt{3}\bar{u}_{i+1}^{(1)}(-2+\xi) + 6\sqrt{3}\bar{u}_{i+1}^{(0)}(-3+2\xi) + 3u_{i+2}^{(0)}(-3+2\xi)(-7-2\sqrt{3}+2\xi)\big)$$
$$\big/ \big(63 - 60\xi + 12\xi^2\big), \tag{D.104}$$

$$p_2(x_{i+2+\frac{\sqrt{3}}{6}}) = \big(\sqrt{3}(2u_{i+3}^{(0)} - u_{i+3}^{(1)}) - (3 - \sqrt{3})u_{i+2}^{(0)}(-3+2\xi)\big)/6, \tag{D.105}$$

$$p_3(x_{i+2+\frac{\sqrt{3}}{6}}) = \big(-6\sqrt{3}\bar{u}_{i+1}^{(0)} + \sqrt{3}u_{i+3}^{(0)}(10 - 9\xi + 2\xi^2) + u_{i+2}^{(0)}(105 - 4\sqrt{3} - 9(8 - \sqrt{3})\xi + 2(6 - \sqrt{3})\xi^2)\big)$$
$$\big/ \big(3(35 - 24\xi + 4\xi^2)\big). \tag{D.106}$$

At the point $x_{i+2-\frac{\sqrt{3}}{6}}$, we have:

$$p_1(x_{i+2-\frac{\sqrt{3}}{6}}) = \big(-4\sqrt{3}\bar{u}_{i+1}^{(1)}(-2+\xi) - 6\sqrt{3}\bar{u}_{i+1}^{(0)}(-3+2\xi) + 3u_{i+2}^{(0)}(-3+2\xi)(-7+2\sqrt{3}+2\xi)\big)$$
$$\big/ \big(63 - 60\xi + 12\xi^2\big), \tag{D.107}$$

$$p_2(x_{i+2-\frac{\sqrt{3}}{6}}) = \big(-\sqrt{3}(2u_{i+3}^{(0)} - u_{i+3}^{(1)}) - (3 + \sqrt{3})u_{i+2}^{(0)}(-3+2\xi)\big)/6, \tag{D.108}$$

$$p_3(x_{i+2-\frac{\sqrt{3}}{6}}) = \big(6\sqrt{3}\bar{u}_{i+1}^{(0)} - \sqrt{3}u_{i+3}^{(0)}(10 - 9\xi + 2\xi^2) + u_{i+2}^{(0)}(105 + 4\sqrt{3} - 9(8 + \sqrt{3})\xi + 2(6 + \sqrt{3})\xi^2)\big)$$
$$\big/ \big(3(35 - 24\xi + 4\xi^2)\big). \tag{D.109}$$

Step D.4.2. We find the combination coefficients. For $x_G = x_{i+2+\frac{\sqrt{3}}{6}}$, the associated linear weights are:

$$\gamma_1 = \big((-7+2\xi)(-91 + 3488\sqrt{3} - 30(-1 + 92\sqrt{3})\xi + 528\sqrt{3}\xi^2)\big)$$
$$\big/ \big(6\sqrt{3}(-2+\xi)(8613 - 9204\xi + 3744\xi^2 - 688\xi^3 + 48\xi^4)\big),$$
$$\gamma_2 = \big(29877 + 197\sqrt{3} - 12(3573 + 8\sqrt{3})\xi + 12(1872 + \sqrt{3})\xi^2 - 5136\xi^3 + 432\xi^4\big)$$
$$\big/ \big(9(8613 - 9204\xi + 3744\xi^2 - 688\xi^3 + 48\xi^4)\big),$$
$$\gamma_3 = \big(-117312 + 151\sqrt{3} + (176232 - 386\sqrt{3})\xi - 180(540 - \sqrt{3})\xi^2 + 24(980 - \sqrt{3})\xi^3 - 2112\xi^4\big)$$
$$\big/ \big(18(-17226 + 27021\xi - 16692\xi^2 + 5120\xi^3 - 784\xi^4 + 48\xi^5)\big). \tag{D.110}$$

For $x_G = x_{i+2-\frac{\sqrt{3}}{6}}$, the associated linear weights are:

$$
\begin{aligned}
\gamma_1 &= \big((-7 + 2\xi)(91 + 3488\sqrt{3} - 30(1 + 92\sqrt{3})\xi + 528\sqrt{3}\xi^2)\big) \\
&\quad \big/ \big(6\sqrt{3}(-2 + \xi)(8613 - 9204\xi + 3744\xi^2 - 688\xi^3 + 48\xi^4)\big), \\
\gamma_2 &= \big(29877 - 197\sqrt{3} - 12(3573 - 8\sqrt{3})\xi + 12(1872 - \sqrt{3})\xi^2 - 5136\xi^3 + 432\xi^4\big) \\
&\quad \big/ \big(9(8613 - 9204\xi + 3744\xi^2 - 688\xi^3 + 48\xi^4)\big), \\
\gamma_3 &= \big(-117312 - 151\sqrt{3} + (176232 + 386\sqrt{3})\xi - 180(540 + \sqrt{3})\xi^2 + 24(980 + \sqrt{3})\xi^3 2112\xi^4\big) \\
&\quad \big/ \big(18(-17226 + 27021\xi - 16692\xi^2 + 5120\xi^3 - 784\xi^4 + 48\xi^5)\big).
\end{aligned}
$$

References

[1] R. Abgrall, How to prevent pressure oscillations in multicomponent flow calculations: a quasi-conservative approach, Journal of Computational Physics 125 (1996) 150–160.

[2] R. Abgrall, S. Karni, Computations of compressible multifluids, Journal of Computational Physics 169 (2001) 594–623.

[3] R. Biswas, K.D. Devine, J. Flaherty, Parallel, adaptive finite element methods for conservation laws, Applied Numerical Mathematics 14 (1994) 255–283.

[4] E.H. van Brummelen, B. Koren, A pressure-invariant conservative Godunov-type method for barotropic two-fluid flows, Journal of Computational Physics 185 (2003) 289–308.

[5] A. Burbeau, P. Sagaut, C.H. Bruneau, A problem-independent limiter for high-order Runge–Kutta discontinuous Galerkin methods, Journal of Computational Physics 169 (2001) 111–150.

[6] R. Caiden, R.P. Fedkiw, C. Anderson, A numerical method for two-phase flow consisting of separate compressible and incompressible regions, Journal of Computational Physics 166 (2001) 1–27.

[7] J.P. Cocchi, R. Saurel, A Riemann problem based method for the resolution of compressible multimaterial flows, Journal of Computational Physics 137 (1997) 265–298.

[8] B. Cockburn, S. Hou, C.W. Shu, The Runge–Kutta local projection discontinuous Galerkin finite element method for conservation laws IV: the multidimensional case, Mathematics of Computation 54 (1990) 545–581.

[9] B. Cockburn, S.Y. Lin, C.W. Shu, TVB Runge–Kutta local projection discontinuous Galerkin finite element method for conservation laws III: one-dimensional systems, Journal of Computational Physics 84 (1989) 90–113.

[10] B. Cockburn, C.W. Shu, TVB Runge–Kutta local projection discontinuous Galerkin finite element method for conservation laws II: general framework, Mathematics of Computation 52 (1989) 411–435.

[11] B. Cockburn, C.W. Shu, The Runge–Kutta local projection P1-discontinuous Galerkin finite element method for scalar conservation laws, Mathematical Modelling and Numerical Analysis (M2AN) 25 (1991) 337–361.

[12] B. Cockburn, C.W. Shu, The Runge–Kutta discontinuous Galerkin method for conservation laws V: multidimensional systems, Journal of Computational Physics 141 (1998) 199–224.

[13] R.P. Fedkiw, T. Aslam, B. Merriman, S. Osher, A nonoscillatory Eulerian approach to interfaces in multimaterial flows (the ghost fluid method), Journal of Computational Physics 152 (1999) 457–492.

[14] G.S. Jiang, C.W. Shu, Efficient implementation of weighted ENO schemes, Journal of Computational Physics 126 (1996) 202–228.

[15] S. Karni, Multi-component flow calculations by a consistent primitive algorithm, Journal of Computational Physics 112 (1994) 31–43.

[16] B. Koren, M.R. Lewis, E.H. van Brummelen, B. van Leer, Riemann-problem and level-set approaches for homentropic two-fluid flow computations, Journal of Computational Physics 181 (2002) 654–674.

[17] L. Krivodonova, J. Xin, J.F. Remacle, N. Chevaugeon, J. Flaherty, Shock detection and limiting with discontinuous Galerkin methods for hyperbolic conservation laws, Applied Numerical Mathematics 48 (2004) 323–338.

[18] B. Larrouturou, How to preserve the mass fractions positivity when computing compressible multi-component flow, Journal of Computational Physics 95 (1991) 31–43.

[19] X.D. Liu, S. Osher, T. Chan, Weighted essentially nonoscillatory schemes, Journal of Computational Physics 115 (1994) 200–212.

[20] T.G. Liu, B.C. Khoo, C.W. Wang, The ghost fluid method for compressible gas–water simulation, Journal of Computational Physics 204 (2005) 193–221.

[21] T.G. Liu, B.C. Khoo, K.S. Yeo, The simulation of compressible multi-medium flow. Part I. A new methodology with applications to 1D gas–gas and gas–water cases, Computers and Fluids 30 (2001) 291–314.

[22] T.G. Liu, B.C. Khoo, K.S. Yeo, Ghost fluid method for strong shock impacting on material interface, Journal of Computational Physics 190 (2003) 651–681.

[23] J. Qiu, T.G. Liu, B.C. Khoo, Runge–Kutta discontinuous Galerkin methods for compressible two-medium flow simulations: one-dimensional case, Journal of Computational Physics 222 (2007) 353–373.

[24] J. Qiu, T.G. Liu, B.C. Khoo, Simulations of compressible two-medium flow by Runge–Kutta discontinuous Galerkin methods with the ghost fluid method, Communications in Computational Physics 3 (2008) 479–504.

[25] J. Qiu, C.W. Shu, Hermite WENO schemes and their application as limiters for Runge–Kutta discontinuous Galerkin method: one-dimensional case, Journal of Computational Physics 193 (2004) 115–135.

[26] J. Qiu, C.W. Shu, Runge–Kutta discontinuous Galerkin method using WENO limiters, SIAM Journal on Scientific Computing 26 (2005) 907–929.

[27] J. Qiu, C.W. Shu, Hermite WENO schemes and their application as limiters for Runge–Kutta discontinuous Galerkin method II: two-dimensional case, Computers and Fluids 34 (2005) 642–663.

[28] J. Qiu, C.W. Shu, A comparison of trouble cell indicators for Runge–Kutta discontinuous Galerkin method using WENO limiters, SIAM Journal on Scientific Computing 27 (2005) 995–1013.

[29] J. Qiu, B.C. Khoo, C.W. Shu, A numerical study for the performance of the Runge–Kutta discontinuous Galerkin method based on different numerical fluxes, Journal of Computational Physics 212 (2006) 540–565.

[30] W.H. Reed, T.R. Hill, Triangular mesh methods for neutron transport equation, Tech. report LA-UR-73-479, Los Alamos Scientific Laboratory, 1973.

[31] C.W. Shu, TVB uniformly high-order schemes for conservation laws, Mathematics of Computation 49 (1987) 105–121.

[32] C.W. Shu, Essentially nonoscillatory and weighted essentially nonoscillatory schemes for hyperbolic conservation laws, in: A. Quarteroni (Ed.), Advanced Numerical Approximation of Nonlinear Hyperbolic Equations, in: Lecture Notes in Mathematics, CIME subseries, Springer-Verlag, Berlin/New York, 1997, ICASE Report 97-65.

[33] C.W. Shu, S. Osher, Efficient implementation of essentially nonoscillatory shock capturing schemes, Journal of Computational Physics 77 (1988) 439–471.

[34] E.F. Toro, Riemann Solvers and Numerical Methods for Fluid Dynamics, a Practical Introduction, Springer, Berlin, 1997.
[35] E.F. Toro, M. Spruce, W. Speares, Restoration of the contact surface in the Harten–Lax–van Leer Riemann solver, Shock Waves 4 (1994) 25–34.
[36] J. Zhu, J. Qiu, A class of the fourth order finite volume Hermite weighted essentially nonoscillatory schemes, Science in China Series A: Mathematics 51 (2008) 1549–1560.
[37] J. Zhu, J. Qiu, Hermite WENO schemes and their application as limiters for Runge–Kutta discontinuous Galerkin method III: unstructured meshes, Journal of Scientific Computing 39 (2009) 293–321.
[38] J. Zhu, J. Qiu, C.W. Shu, M. Dumbser, Runge–Kutta discontinuous Galerkin method using WENO limiters II: unstructured meshes, Journal of Computational Physics 227 (2008) 4330–4353.